5. DATA ANALYSIS TECHNIQUES

Trajectory analyses have historically been used to trace the path of polluted air masses prior to their arrival at a given receptor site. Such analyses, by linking downwind measurements of ambient air quality with specific geographic areas upwind, can be very helpful in exploring the relative contribution of transported emissions from potential source regions on high and low pollution days. As with all of the tools and modeling techniques discussed in this report, trajectory analysis is not without some uncertainties and limitations. One such limitation is the fact that these analyses are typically unable to distinguish emission contributions from one point along the length of the trajectory from a different point along the path. In addition, the accuracy of any individual back trajectory calculation for a single observation or episode may be compromised by inherent limitations in the underlying Lagrangian trajectory models, which tend to become less accurate as the calculation progresses further back in time. Fortunately, a variety of techniques are available to mitigate these uncertainties and enhance confidence in the results obtained using trajectory analysis. These include techniques for triangulating results across multiple sites, ensemble techniques that combine the results of large numbers of back trajectories, clustering algorithms that group similar trajectories based on their spatial characteristics, and techniques for combining trajectory analyses with source apportionment models. All of these strategies can be useful in improving and refining traditional trajectory analyses.

This chapter describes the results of back trajectory analyses that have been conducted to date for key pollutant species observed at MANE-VU and nearby receptor sites. In addition, we explore novel techniques for improving the accuracy of individual trajectories by grouping meteorologically similar back-trajectories into trajectory "clusters" and examining the relationship between the transport pathways defined by these clusters and downwind air quality observations. We then turn to source apportionment models which can be used to group available monitoring data for various components of $PM_{2.5}$ in logical combinations that best explain the variation in observed species concentrations in terms of specific "source profiles." These source profiles are used to distinguish the emissions from common pollution sources (e.g., mobile sources, coal combustion). The information obtained through source apportionment analysis can then be used in combination with back trajectory analysis to link specific geographic source regions with downwind air quality conditions and to establish the relative contribution of different source regions to visibility impacts at the receptor site.

This chapter provides further description of several trajectory analysis techniques, before proceeding to a review of the insights gained to date by applying these techniques to analyze source regions for particulate pollution in the MANE-VU region. Preliminary results and interpretation are presented and used to support and bolster the basic conceptual model of regional haze outlined in Chapter 2.

5.1. Trajectory Analysis

The Hybrid Single Particle Lagrangian Integrated Trajectory (HYSPLIT) model (Draxler, 1997 and 1998) was used to calculate back trajectories for 13 sites in the northeastern United States. Most of these sites are located in Class I areas that are

subject to the Haze Rule, but several others are located in areas where potential nonattainment with the $PM_{2.5}$ NAAQS warrant analysis. Back trajectories were calculated eight times per day for starting heights of 200, 500, and 1,000 meters above ground level using meteorological wind fields for the five-year period from 2000 through 2004. Meteorological data from the National Oceanic and Atmospheric Administration (NOAA) Air Resources Laboratory (ARL) archives were used. These include wind fields from the Eta Data Assimilation System (EDAS), which cover North America with an 80 km spatial resolution and are based on 3-hourly variational analyses (Rolph, 2003). For the analyses presented here, we exclusively used the 500 meter EDAS trajectories from the baseline period (2000-2004).

Each trajectory was matched with corresponding monitoring data collected as close in time as possible to the "start" time of the back trajectory calculation. The analysis included ambient measurements for $PM_{2.5}$ and ozone (O_3), as well as all particulate matter constituents that are routinely measured as part of the IMPROVE program.

The resulting database of air quality monitoring results and associated back trajectories was used to develop several statistical measures of the probability or likelihood that a given upwind source region is associated with good or poor air quality at the receptor sites analyzed. Appendix A provides a detailed description of the metrics that were developed for this purpose and how they were calculated using both traditional trajectory analysis and cluster analysis techniques. This appendix also provides site-specific results.

5.1.1. Incremental Probability

The incremental probability (IP) field represents a measure of the likelihood that a given source region contributes more than "average" to high concentrations of a particular pollutant at a downwind receptor site (see Appendix A for a more complete definition). This technique can also be used to identify locations that are *less* likely to contribute to poor air quality at a given receptor site, thus allowing for more robust conclusions to be drawn about likely source regions for individual fine particle constituents.

Calculating IP fields for a subset of back trajectories within a complete sample can help further illuminate the different roles of different source regions. For example, it is interesting to note distinct differences between the IP field for back trajectories corresponding to the 10 percent highest observed sulfate values in the Northeast (three sites are shown that bracket the MANE-VU region's Class I sites) and the IP field for trajectories corresponding to the lowest sulfate values in the Northeast (specifically, sulfate values in the lowest 10th percentile). Figure 5-1 and Figure 5-2 illustrate the IP fields for each set of observations, respectively.

In Figure 5-1 and Figure 5-2, note that the red color indicates areas with greater probability of contributing to transport on the selected days. These show that the very highest observed sulfate values across the region are strongly associated with transport from a source region that encompasses the Ohio River Valley, western Pennsylvania, and

the urban East Coast corridor. On the days with the lowest measured sulfate, transport is associated with northwesterly winds from Canada and weather patterns off the Atlantic.

Figure 5-1. Incremental Probability (Top 10% Sulfate) at Acadia, Brigantine and Lye Brook 2000-2004

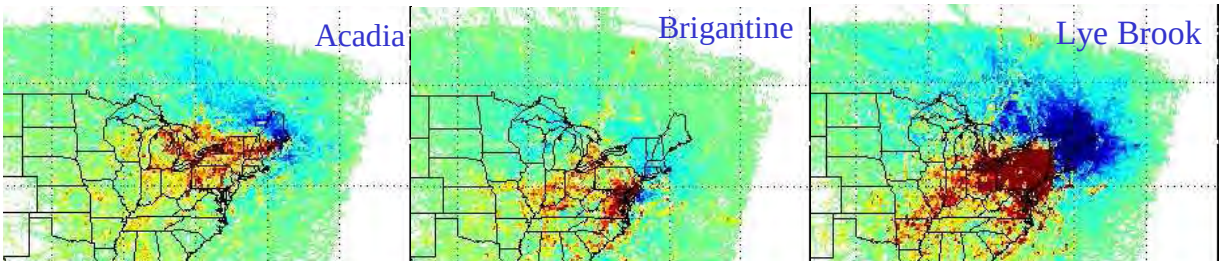

Figure 5-2. Incremental Probability (Bottom 10% Sulfate) at Acadia, Brigantine and Lye Brook 2000-2004

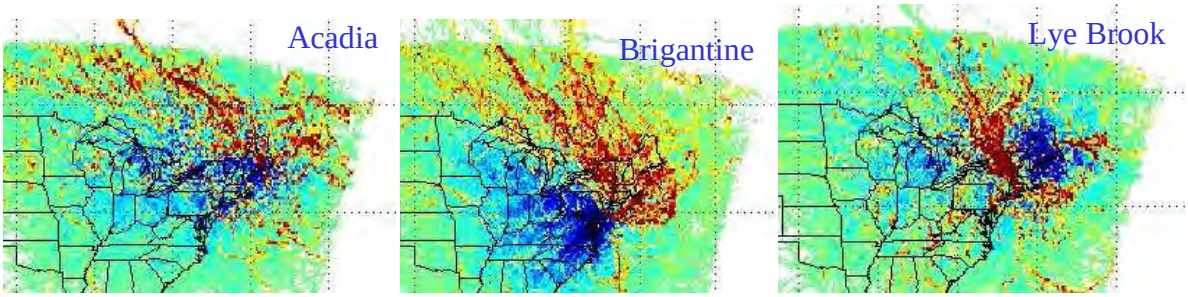

5.1.2. Clustered Back-Trajectories

Each of the IP fields shown in Figure 5-1 or Figure 5-2 incorporate results from over 14,000 back trajectories over the five-year period analyzed. In cases like these, where IP fields are calculated from a very large set of data points, the error in the calculation of any individual trajectory — which can be as high as 30 percent or more of the total transport distance involved in a given trajectory — is not likely to affect the overall result. Assuming that such errors are randomly distributed (i.e., no systematic bias exists in the calculations used by the trajectory model to calculate wind speed or direction), the use of large numbers of individual trajectories will effectively ensure that the random errors cancel out. To further minimize the effect of any errors with respect to individual trajectories, it is also possible to cluster large numbers of back trajectories according to their three-dimensional similarity (see Appendix A for a detailed description of several methodologies used). Figure 5-3 shows residence-time probability fields for clusters of similar back trajectories grouped according to their proximity to unique meteorological pathways. This metric yields probabilistic representations of the meteorological pathways which were most likely to be associated with the highest observed sulfate concentrations at the receptor site. Such probabilistic representations reduce the reliance on any one back trajectory and ensure that the general pattern used to associate a transport pathway with a downwind receptor site is more likely to be accurate.

Figure 5-3. Proximity based cluster with the highest associated sulfate value for three sites in the MANE-VU region, Acadia (sulf=3.19 μg/m^3), Brigantine (sulf=6.79 μg/m^3), and Lye Brook (sulf=3.92 μg/m^3)

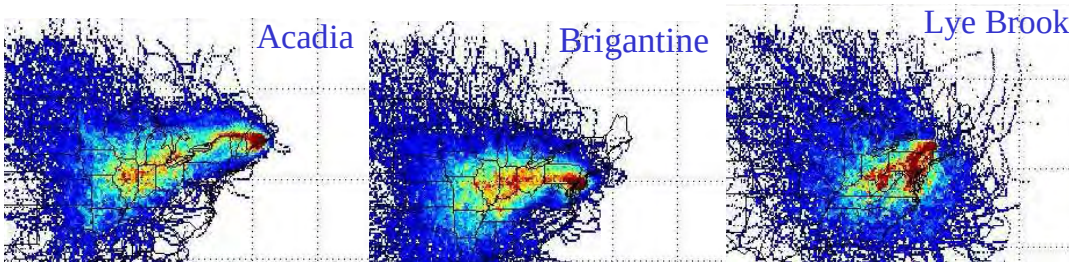

5.1.3. Cluster-Weighted Probability

The clusters derived above can be used individually or combined in an "ensemble cluster" approach similar to how individual trajectories are combined to develop the IP metric. This second method for associating transport patterns with downwind pollution measurements involves using all clusters generated by the clustering algorithms described in the preceding section (and in detail in Appendix A) and weighting them by their average observed sulfate value. Simply averaging the residence-time probability of all clusters would yield the "everyday" probabilities that are used in calculating IP fields. Instead, weighting each cluster *before* the averaging process serves to highlight transport patterns that are associated with high sulfate levels at the receptor site, while downplaying patterns that are associated with low values. Figure 5-4 shows the resulting cluster-weighted probability (CWP) field. Results are similar to those obtained using the incremental probability metric described previously, but they now include all clusters, not just the high-day values.

A noteworthy feature of the clustering process is that while it reduces uncertainty about prevailing transport patterns, it is not helpful in taking advantage of weather variations to identify specific source regions. Thus, results for a particular site should be interpreted as showing that observed air quality conditions have an increased probability of being associated with the transport of a specific pollutant, as opposed to being associated with a particular source region for a given pollutant. Put another way, it is difficult to make an association with a specific point along the pathway defined by a cluster. As with the IP approach described earlier, however, multi-site averaging can address this ambiguity by making it possible to triangulate on regions that are associated with the transport of pollution to multiple sites in different locations, as shown in Figure 5-4.

Both trajectory-based approaches (i.e., IP and CWP) have also been applied to Class I receptor sites in the nearby VISTAS region, which includes the Dolly Sods and Otter Creek Wilderness Areas in West Virginia as well as Shenandoah National Park and the James River Face Wilderness Area in Virginia. Results for the VISTAS Class I sites are presented at the conclusion of Appendix A.

Figure 5-4. Cluster Weighted Probability at Acadia, Brigantine and Lye Brook 2000-2004

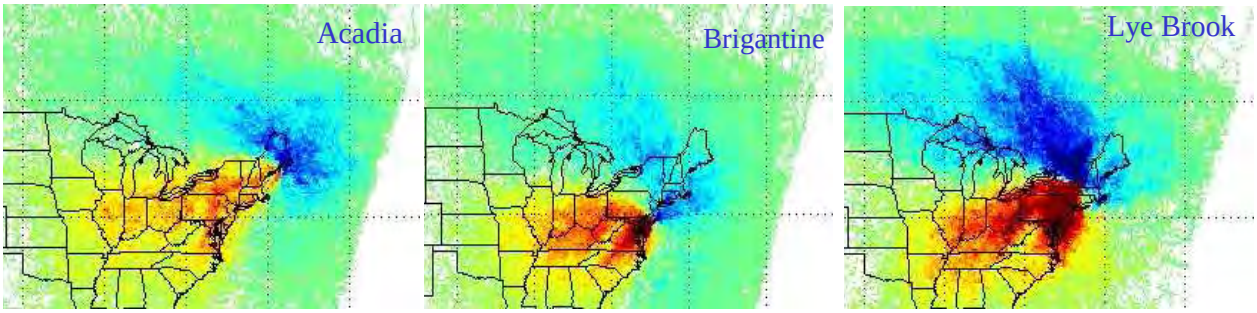

5.2. Source Apportionment Models and Ensemble Trajectory Analysis of Source Apportionment Results

Previous sections of this chapter have discussed a category of receptor-based assessment techniques known more generally as ensemble trajectory analysis. The latter category includes residence time analysis (RTA) as well as potential source contribution function (PSCF) and cluster analysis (see also Appendix A). In this section we turn to multivariate mathematical models for analyzing source contributions, such as chemical mass balance (CMB) models, principal component analysis (PCA), positive matrix factorization (PMF), and UNMIX.

Receptor-based models begin with ambient air quality measurements at one or more receptor locations and work "backward" to identify logical combinations of pollutant species that best fit a "source profile." Sources matching that profile are assumed to have contributed to the ambient pollutant concentrations historically observed at the receptor locations. These models are typically driven by variations in PM constituent concentrations across multiple observations at one or more sites. An advantage of PCA, PMF, and UNMIX is that source profiles do not need to be known in advance; however, this does mean that the results must be subjectively interpreted to identify and distinguish likely sources.

Because of these complexities and because the multivariate models typically rely entirely on measurements of PM constituents without regard to meteorology, it can be extremely useful to consider results obtained through the ensemble trajectory techniques (which rely on meteorology only) when interpreting or evaluating the outputs from a multivariate modeling exercise.

Appendix B provides details of numerous source apportionment and associated ensemble back trajectory analyses. These details cover results obtained for many of the most significant components of fine particulate mass and resulting light extinction. Here we focus on the "secondary sulfate" or "coal" source profile that was identified at nearly every site in the eastern United States. Secondary sulfate typically accounts for 30–60 percent of overall fine particle mass and 60–80 percent of visibility impairment on the haziest days in the Northeast.

Figure 5-5 shows results from one of the broadest studies conducted to date of sulfate sources and characteristics at nine eastern IMPROVE sites. The bars on the left

show the fraction of total sulfate measured at each site that is contributed by the "sulfate/coal" source profile as determined by the source apportionment models. The bars on the right show the fraction of each "sulfate/coal" source profile that is composed of sulfate. Figure 5-5 suggests that: (1) large sources contribute 70–90 percent of the total sulfate measured at these sites, and (2) that the contribution from these large sources consists of 50–90 percent sulfate.

Figure 5-5. Sulfate characteristics of "secondary sulfate" (coal) sources identified at eastern sites

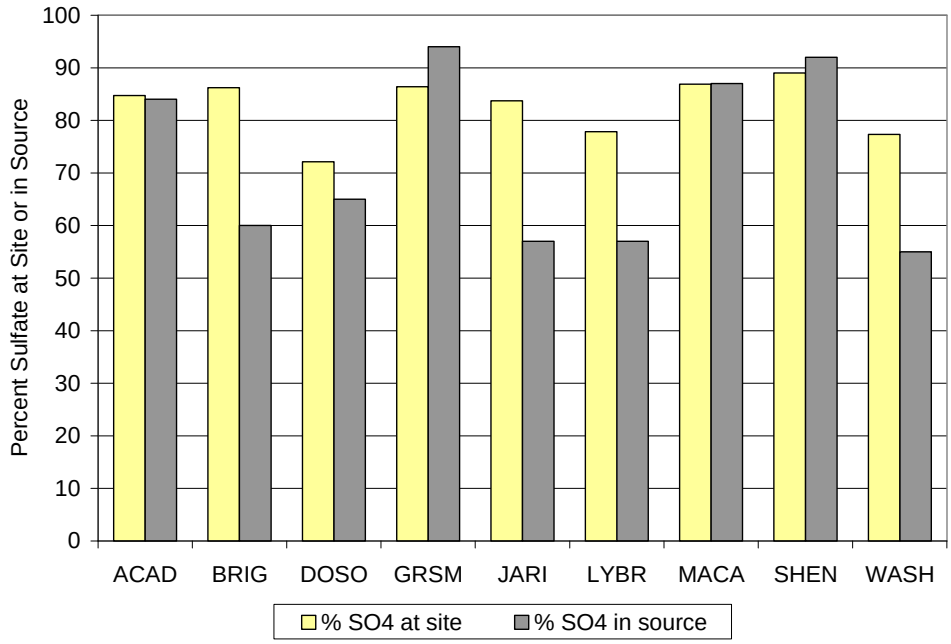

When large sulfate sources are associated with upwind states or regions through the use of back trajectories (Figure 5-6), it becomes clear that many Class I and urban sites in MANE-VU and adjoining areas are influenced by a common source region. These findings suggest that reductions in coal-related SO_2 emissions would have substantial benefits in terms of improved visibility and reduced PM concentrations over a large part of the eastern United States and eastern Canada.

This conclusion is further reinforced by comparing regions with significant emissions that match the "source profiles" generated by available mathematical modeling tools to regions identified through trajectory analysis as having a high probability of being upwind on days with high sulfate levels and high reconstructed extinction values. As shown in Figure 5-6, the degree of correspondence between these regions is substantial. This indicates that the "secondary sulfate/coal combustion" source profile prominent at several eastern sites is strongly linked to regions associated with the highest 10 percent of recorded sulfate and reconstructed extinction values. It is noteworthy that the upwind regions identified in Figure 5-7 are derived from measurements spanning the entire IMPROVE network, suggesting that the source region for "secondary sulfate/coal combustion," which is a dominant contributor to visibility impairment in parts of the eastern United States, is also a major contributor to observed sulfate and extinction outside the MANE-VU region.

Figure 5-6. Incremental Probabilities for "Secondary Sulfate" (Coal) Sources in Eastern U.S.

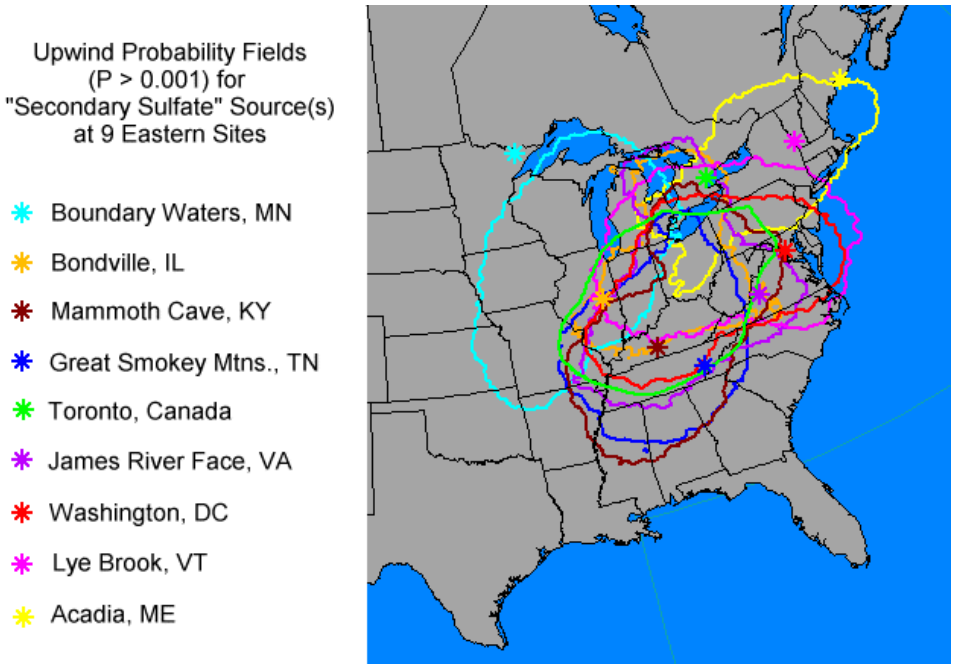

5.3. Trajectory Model Evaluation and Future Work

The geographical correspondence exhibited in Figure 5-7 extends to the multi-site average IP fields calculated for the MANE-VU region and shown previously in Figure 5-1. It also extends to the multi-site average IP field calculated using the ATAD model and shown in Figure B-30 in Appendix B. Essentially, both figures are versions of the same thing, but they do exhibit some subtle differences. These differences are highlighted in Figure 5-8 which compares the results of ATAD and HYSPLIT IP calculations for the top 10 percent of sulfate, selenium, and nickel observations at Lye Brook, Vermont. Sulfate is a secondary pollutant that tends to peak in the summer, whereas nickel and selenium are primary pollutants that typically peak in the wintertime. Ni and Se serve as excellent markers for residual oil and coal combustion respectively. The figure indicates strong agreement between the two models in terms of

Figure 5-7. Comparison of probability fields for observed sulfate, "sulfate" source profiles for seven eastern sites and reconstructed deciviews

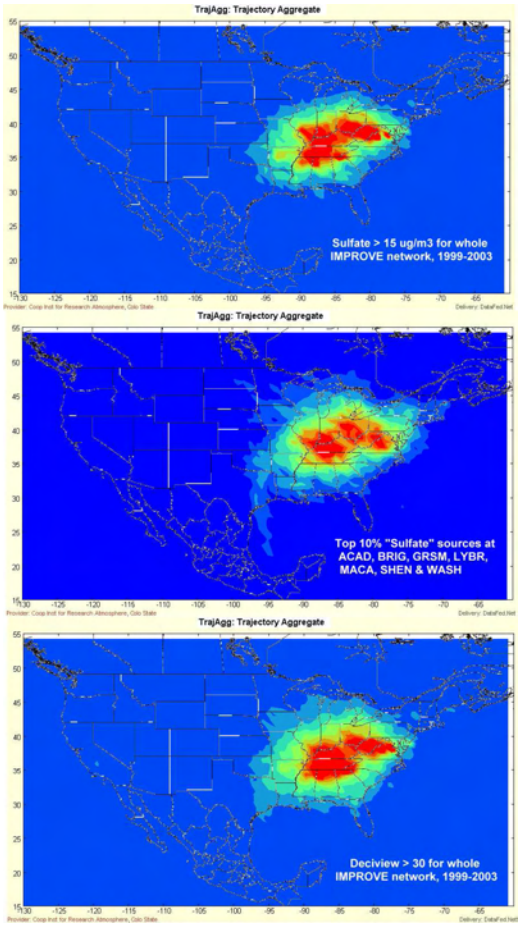

the IP fields they calculate for nickel, suggesting that — during wintertime — primary pollutants are tracked well by both techniques. There is less agreement between the IP fields for sulfate, suggesting either a southerly bias to the HYSPLIT calculations for this secondary pollutant, or a westerly bias to the ATAD results.

Seasonal differences in the meteorology that affects Lye Brook and other East Coast sites during the summer versus during the winter may help to explain these model discrepancies. Some of the largest absolute differences between the ATAD and HYSPLIT estimates occur for the highest sulfate days. While there are many differences between the models, one key difference is in their trajectory start heights. The HYSPLIT trajectories all start at 500 meters above ground level while the ATAD model first estimates a "transport layer depth" (TLD) and then initiates the trajectory (while constraining subsequent trajectory endpoints) at a point roughly half way between ground level and the TLD. During summer, when the largest sulfate events occur, the resulting ATAD start heights are roughly twice as high as the 500 m HYSPLIT start heights (see Figure 5-9). Hence the ATAD calculations tend to extend over a greater distance to the west, while the summer HYSPLIT trajectories may be more reflective of flows that are nearer the surface and more frequently east of the Appalachian Mountains. Both flow regimes are important. In fact, Blumenthal et al. (1997) have observed that the highest ozone concentrations in the Northeast (which often coincide with episodes of high sulfate concentrations) tend to occur when surface flows up the Northeast urban corridor combine with synoptic flows over the Appalachian Mountains from the west, a pattern that is often accompanied by lower level nocturnal jets along the Northeast corridor and through gaps in the Appalachians.

Figure 5-8. Comparison of IP contours generated by ATAD and HYSPLIT (both EDAS and FNL) for sulfate, nickel and selenium at Lye Brook

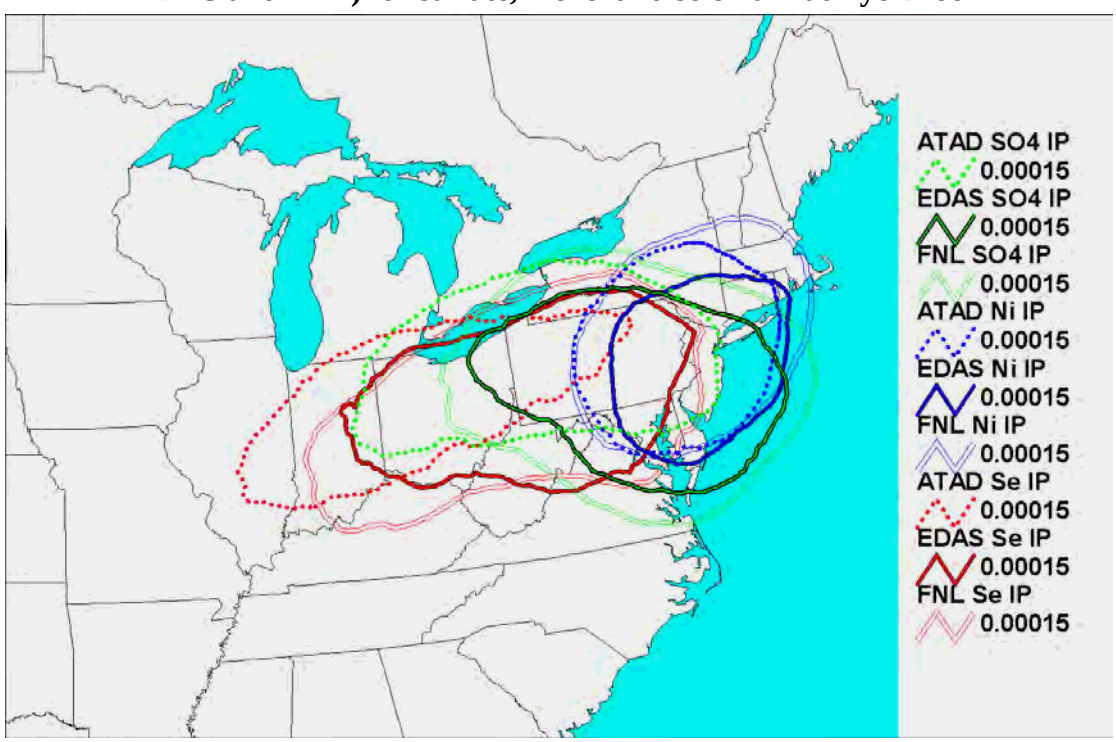

An extensive evaluation of the performance of HYSPLIT, ATAD, and Capita Monte Carlo trajectory models using a variety of different meteorological drivers, ensemble trajectory techniques, and performance tracers was recently conducted as part of the Big Bend Regional Aerosol and Visibility Observational (BRAVO) study (Pitchford et al., 2004). No one model consistently out-performed the others at that site, hence results from these and more sophisticated photochemical grid models (REMSAD and CMAQ) were merged to produce a best-estimate, "consensus" apportionment of sulfate in the BRAVO study.

MANE-VU is using all available trajectory models, trajectory-related metrics, and improved understanding of transport phenomena to further explore and support the development of emission control strategies for reducing regional haze.

Figure 5-9. ATAD Transport Layer Depth (TLD) by month. Color indicates the length of time prior to arriving at the receptor.

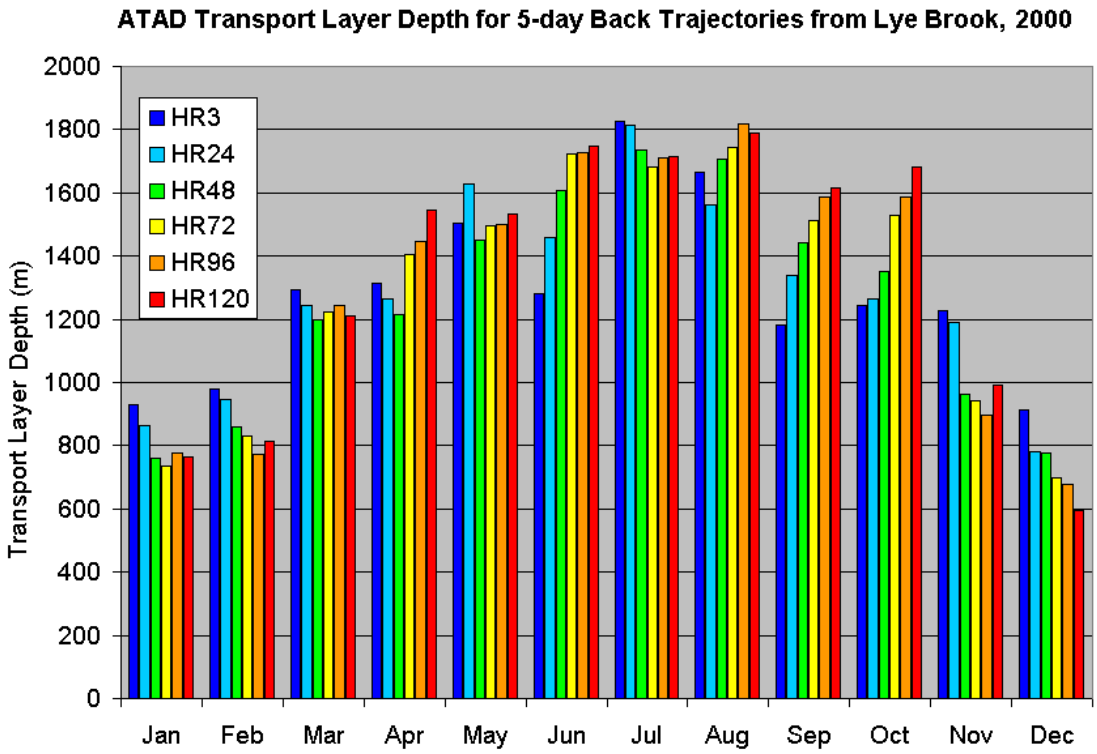

References

Blumenthal, D.L., Lurmann, F.W., Kumar, N., Ray, S.E, Korc, M.E., Londergan, R., Moore, G., Transport and mixing phenomena related to ozone exceedances in the Northeast U.S. Working Draft No. 1.1 prepared for Ozone Transport Assessment Group Air Quality Analysis Workgroup by Sonoma Technology, Inc., Santa Rosa, CA and Earth Tech, Concord, MA, STI-996133-1710-WD1.1, February 1997.

Draxler, R.D. and Hess, G.D., "Description of the HYSPLIT-4 Modeling System," *NOAA Technical Memorandum ERL, ARL-224*, Air Resources Laboratory, Silver Springs, Maryland, 24 pgs., 1997.

Draxler, R.D. and Hess, G.D., "An Overview of the HYSPLIT-4 Modelling System for Trajectories, Dispersion, and Deposition," *Australian Meteorological Magazine*, 47, 295-308, 1998.

Pitchford, M.L., Schichtel, B.A., Gebhart, K.A., Barna, M.G., Malm, W.C., Tombach, I.H., and Knipping, E.M., "Causes of Haze at Big Bend National Park – Results of the BRAVO Study and More" Regional and Global Perspectives on Haze: Causes, Consequences and Controversies – Visibility Specialty Conference, Air & Waste Management Association, Asheville, NC October 25-29, 2004.

Rolph, G.D., Real-time Environmental Applications and Display sYstem (READY) Website (http://www.arl.noaa.gov/ready/hysplit4.html). NOAA Air Resources Laboratory, Silver Spring, MD., 2003.

6. CHEMICAL TRANSPORT MODELS

Eulerian or "grid" models have traditionally served as the workhorse of air quality planning programs. These tools strive to be comprehensive in accounting for emissions, meteorological dynamics, chemical production, transformation, and destruction as well as wet and dry deposition and microphysical processes. With this degree of sophistication comes attendant uncertainty. Many of the more complex processes (e.g., cloud processes and boundary layer dynamics) are handled through parameterizations that attempt to approximate the real atmosphere at an appropriate level of detail. Chemical transport models for ozone and fine particles have improved markedly over the past several years as various groups have developed competing models and as the different strengths and weaknesses of these models help to shed light on various aspects of the underlying science.

Two regional-scale air quality models have been evaluated and used by NESCAUM to perform air quality simulations. These are the Community Multi-scale Air Quality modeling system (CMAQ)[30] and the Regional Modeling System for Aerosols and Deposition (REMSAD).[31] Appendix C provides detailed descriptions of these models and of their use by NESCAUM, together with performance evaluations and preliminary results. A brief overview of the two modeling platforms in terms of their relevance to future SIP work is provided here, along with highlights of the findings.

6.1. Chemical Transport Model (CTM) platforms – Overview

Both REMSAD and CMAQ are being used with a 12 km grid[32] in the eastern U.S. domain (see Figure 6-1(b)). Air quality is modeled on 22 vertical layers with hourly temporal resolution for the entire calendar year 2002. REMSAD has simplified chemistry but allows for emissions tracking of sulfate, nitrate, and mercury through a tagging feature that calculates the contribution of specific sources to ambient concentrations, visibility impacts, and wet or dry deposition. REMSAD has shown good performance when reproducing annual or seasonal statistics for sulfate and mercury chemistry, while CMAQ has shown good performance for multiple species. A new release of CMAQ (version 4.5) may improve performance for sulfate, nitrate and organics over what Appendix C presents and will be used with the quality-assured meteorology and emission inventory inputs described below for final SIP submissions in 2007 or 2008.

Meteorological inputs have been developed by the University of Maryland (UMD) using the Fifth-Generation Pennsylvania State University/National Center for Atmospheric Research (NCAR) Mesoscale Model (MM5) system.[33] A modified Blackadar boundary layer scheme is used as well as physics options including explicit representations of cloud physics with simple ice microphysics (no mixed-phase processes) and the Kain-Fritsch cumulus parameterization.

---

[30] See Byun and Ching, 1999.
[31] See ICF/SAI, 2002.
[32] 12 km grid describes a 12 by 12 km grid cell
[33] http://www.mmm.ucar.edu/mm5/

The New York Department of Environmental Conservation and NESCAUM are processing emissions inputs using the Sparse Matrix Operator Kernel Emissions (SMOKE) Modeling System. To model biogenic emissions, SMOKE uses the Biogenic Emission Inventory System, version 2.3 (BEIS2) and version 3.09 and 3.12 (BEIS3). SMOKE has also been integrated with the MOBILE6 model for on-road emissions. MANE-VU has developed a quality-assured 2002 emissions inventory which is being merged with the regional inventories for other RPOs in order to provide a comprehensive emissions inventory for the entire Northeast domain shown in Figure 6-1(b).

A dynamic 3-dimensional boundary condition feeds ambient concentration fields in at the domain boundaries which are representative of actual concentrations during 2002. This dynamic boundary condition was developed by applying the output of a global model run (Park et al., 2004) with 4 degree longitude by 5 degree latitude horizontal resolution at the boundaries of the 36 km grid domain shown in Figure 6-1(a). The results of this annual simulation are then applied at the boundary of our 12km grid domain, ensuring acceptable representation of the general trends and sulfate patterns that were present during the simulation period.

Figure 6-1. Modeling domains used in NESCAUM air quality modeling studies. (a) Domain 1: 36 km National US grid domain with location of 12 km grid domain highlighted; (b) Domain 2: 12km Northeast US grid domain. The gridlines are shown at 180 km intervals (5 x 5 36 km cells or 15 x 15 12 km cells).

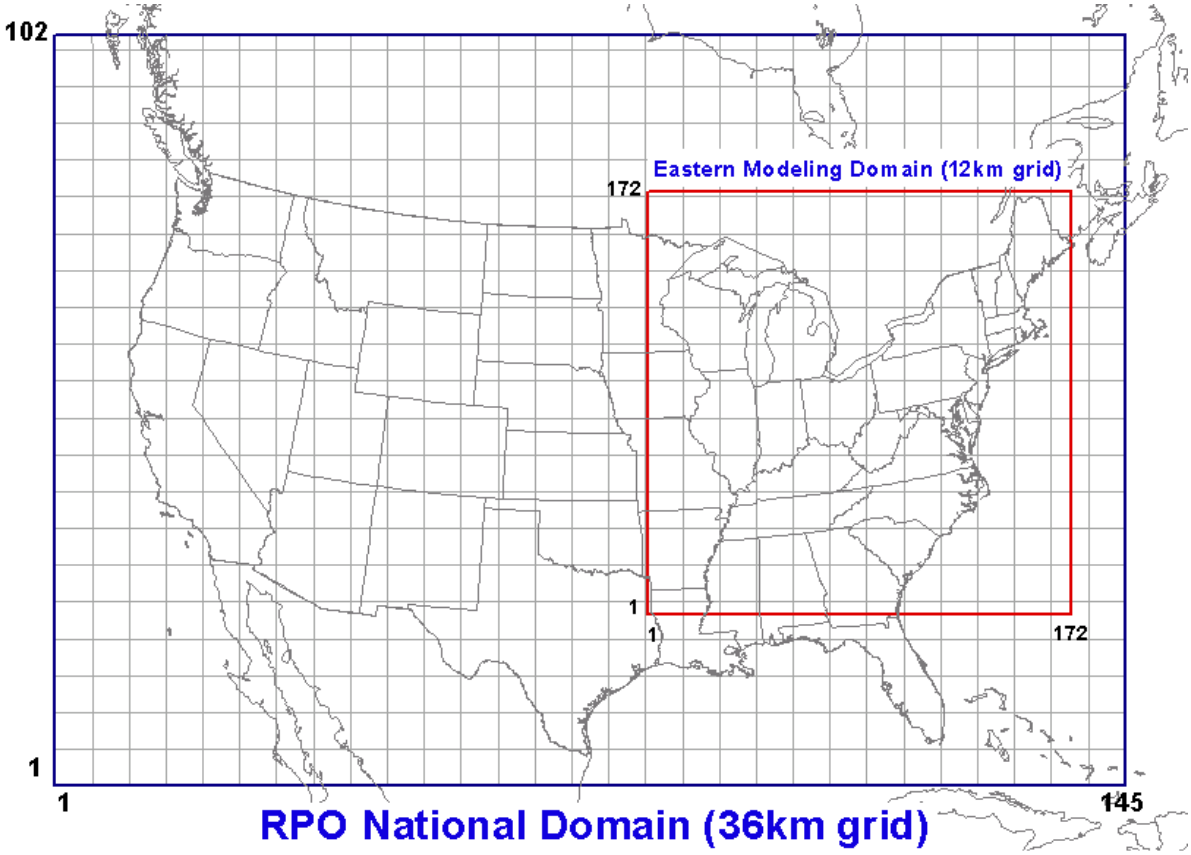

6.2. Preliminary Results

CMAQ has been run for a complete set of baseline simulations including 2002, 2009 and 2018. These preliminary runs are described in greater detail in Appendix C, but include inventory and meteorological drivers which will be updated for final SIP submissions. Nonetheless, these preliminary results suggest that implementation of existing regulations (including USEPA's Clean Air Interstate Rule, or CAIR) will continue to yield significant improvements in visibility over the next decade, primarily as a result of regional sulfate reductions (See Figure 6-2 a and b below for visibility improvement and see Figure C-27 in Appendix C for sulfate mass reductions). Despite these potential improvements, not all MANE-VU Class I areas are anticipated to achieve uniform progress goals as described by current USEPA guidance.[34] Brigantine Wilderness Area in New Jersey is projected to fall about a half deciview short of the uniform rate under existing emission reduction plans.

A significant difference between the CMAQ and the REMSAD results presented here is that NESCAUM has taken the additional step of reprocessing the SO_2 emission sources from each state such that these model inputs are formatted to take advantage of

Figure 6-2(a) and (b): CMAQ Integrated SIP Modeling Platform simulation results for 2002, 2009 and 2018 relative to Uniform Progress Goals calculated according to current USEPA guidance for (a) Northeast Class I sites in MANE-VU and (b) Mid-Atlantic Class I sites in or near MANE-VU.

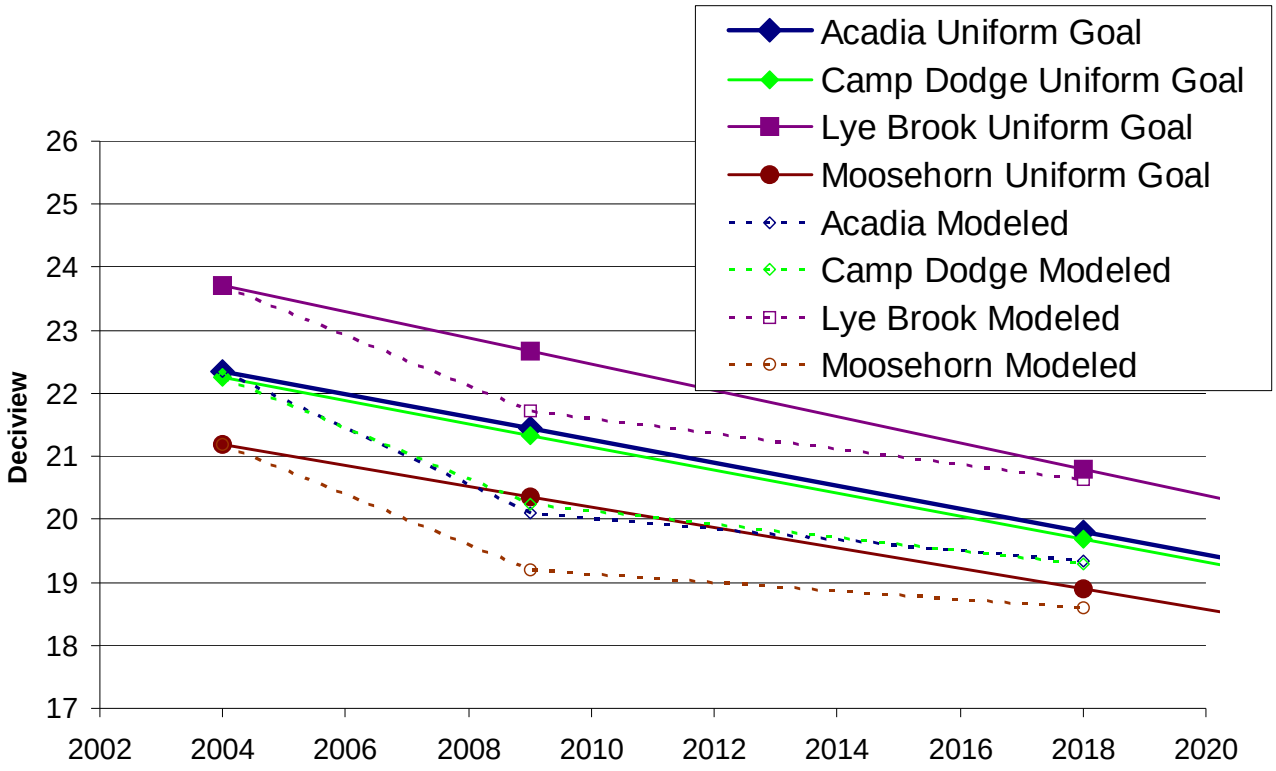

[34] We note that uniform progress goals do not necessarily dictate visibility levels required by statute, but do represent a point of comparison for states when establishing *reasonable* progress goals toward our national visibility goal of no anthropogenic visibility impairment by 2064.

Figure 6-2(b).

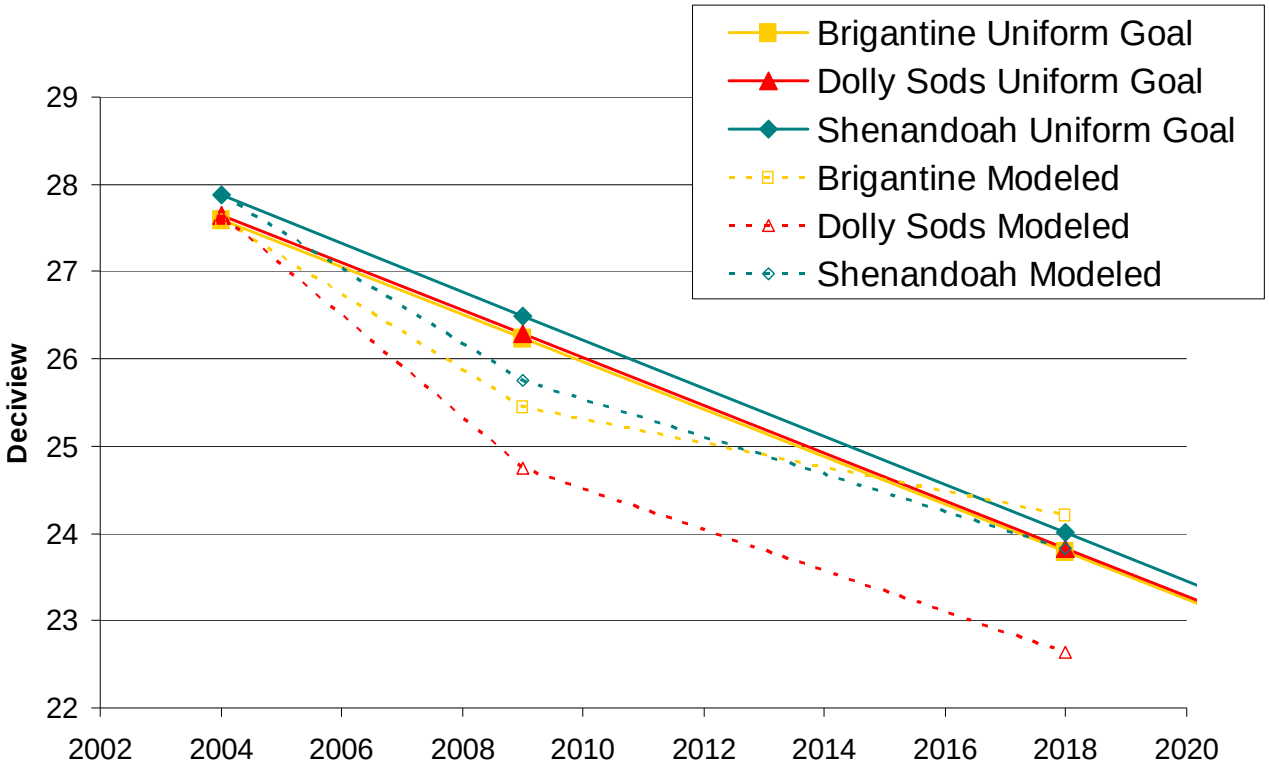

REMSAD's tagging capabilities. Thus, all SO_2 emissions included in the model for the eastern half of the country, Canada and the boundary conditions have been tagged according to state of origin. This allows for a rough estimation of the total contribution from elevated point sources in each state to simulated sulfate concentrations at eastern receptor sites. The tagging scheme employed for this analysis is illustrated in Figure 6-3. Using identical emission and meteorological inputs to those prepared for the Integrated SIP (CMAQ) platform, REMSAD was used to simulate the annual average impact of each state's SO_2 emission sources on the sulfate fraction of $PM_{2.5}$ over the northeastern United States.

Results of these tagged runs indicate that elevated point sources in Pennsylvania, Ohio, and New York contribute significantly, on an annual basis, to sulfate concentrations at all MANE-VU sites. Northern sites (e.g., Acadia) are more influenced by sources in upper midwestern states (e.g., Wisconsin and Michigan) whereas southern sites like Brigantine are more influenced by sources in more southerly states such as West Virginia, Maryland, and Virginia. Shenandoah, a VISTAS Class I site appears to be most strongly influenced by sources in Ohio, Pennsylvania, and West Virginia, followed by other nearby Southeast and Midwest states. Figure 6-4 through Figure 6-7 present these results showing the breakout of sulfate by individual tag. Note that the large "other" fraction of sulfate includes all sources outside the analysis domain, which includes some portions of the VISTAS and CENRAP RPO, Northern and Western Canada in addition to all other (i.e., inter-continental) sources of SO_2. Figure 6-8 shows similar results summarized by RPO for the 20% worst days.

Figure 6-3. REMSAD modeling tagging schemes.
(black: group 1, red: group 2, and blue: group 3)

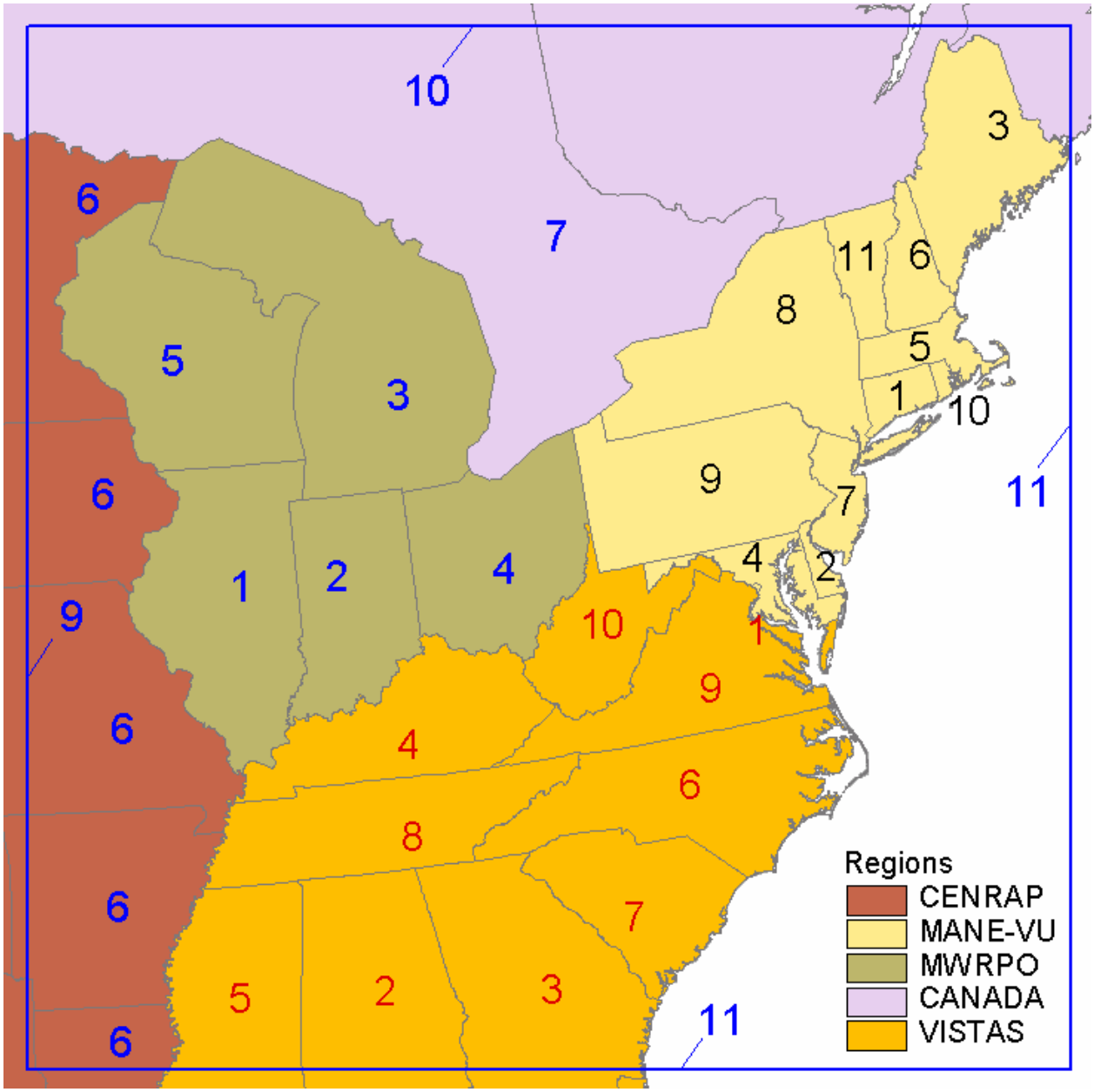

Note: Sulfur species from anthropogenic emission sources are tagged by states for three sets of tags. Tag group 3 also includes boundary conditions. The color of the numbers represents tag groups (black: group 1, red: group 2, and blue: group 3)

Figure 6-4. 2002 Eastern states' contribution to annual PM sulfate in Acadia, ME

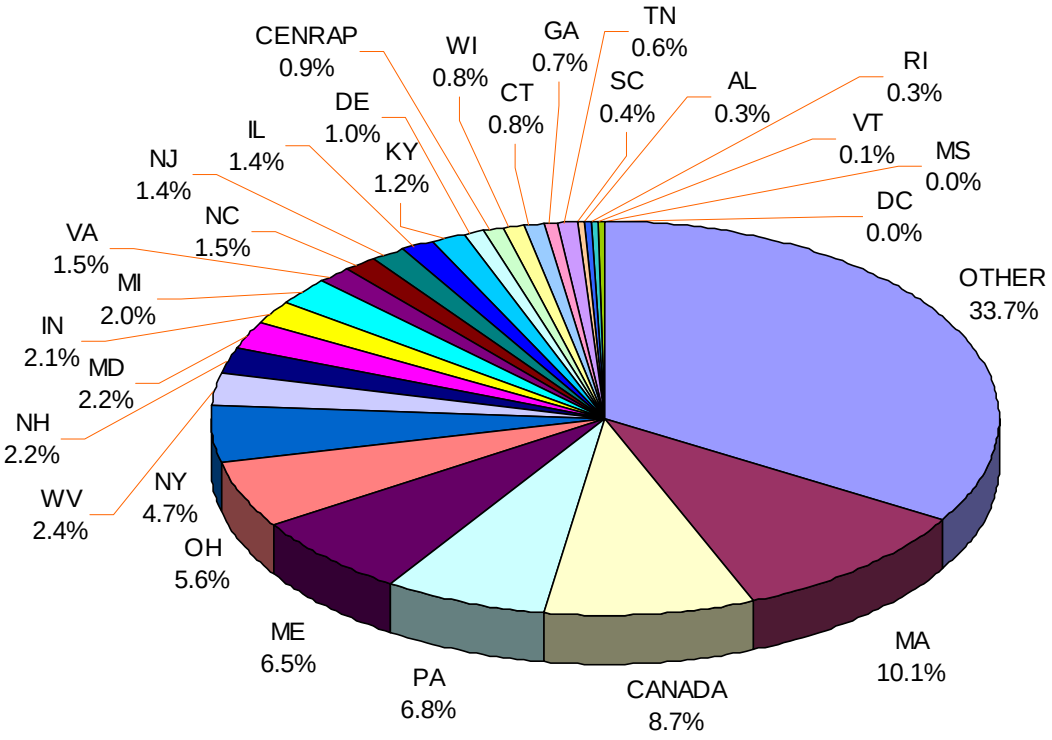

Figure 6-5. 2002 Eastern states' contribution to annual PM sulfate in Brigantine, NJ

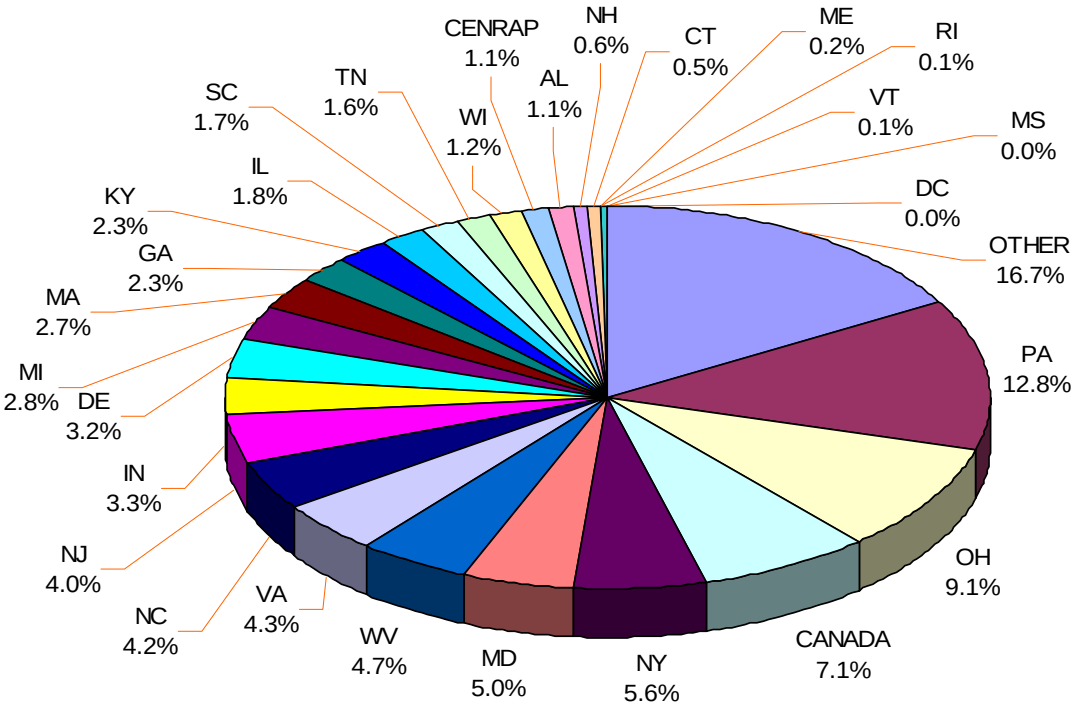

Figure 6-6. 2002 Eastern states' contribution to annual PM sulfate in Lye Brook, VT

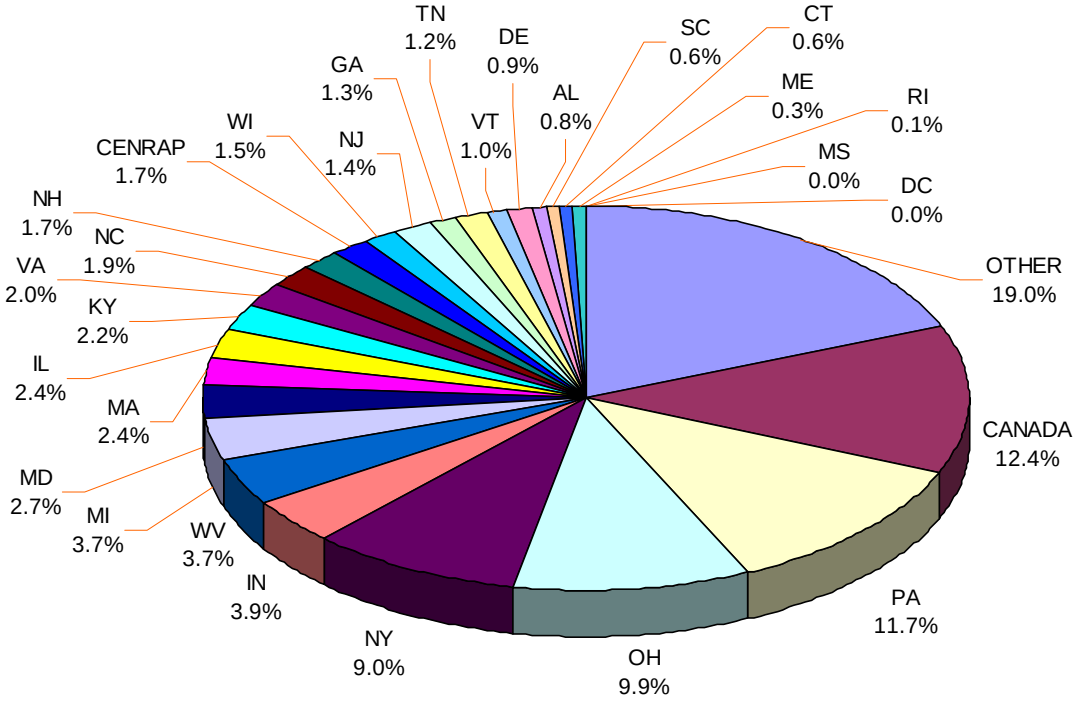

Figure 6-7. 2002 Eastern states' contribution to annual PM sulfate in Shenandoah, VA

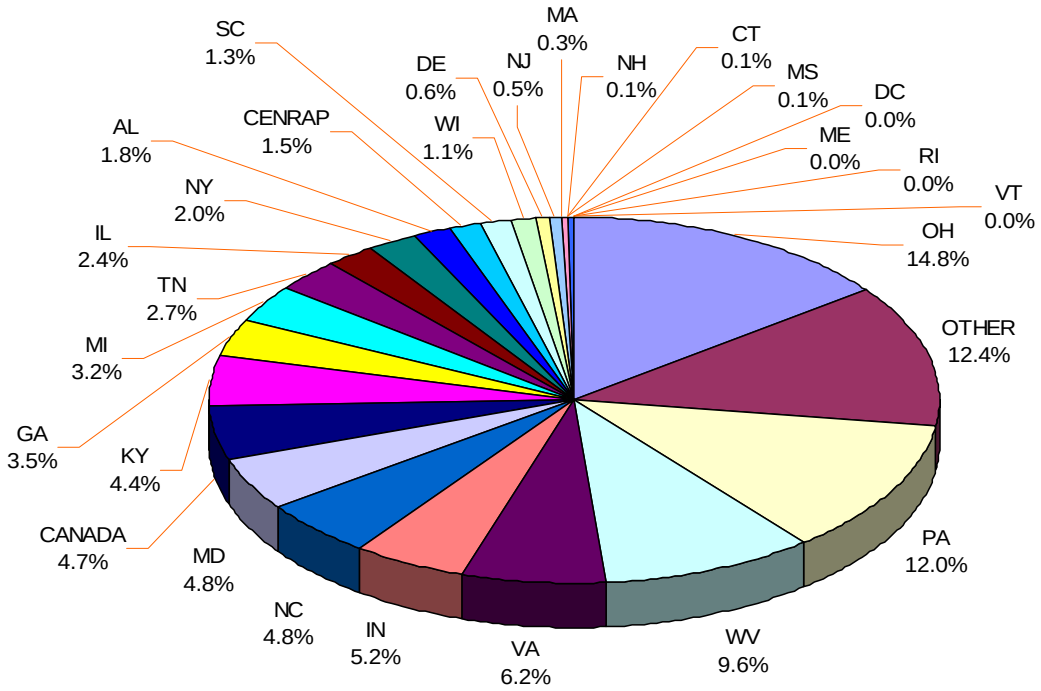

Figure 6-8. Comparison of Sulfate Extinctions on 20% Worst Visibility Days

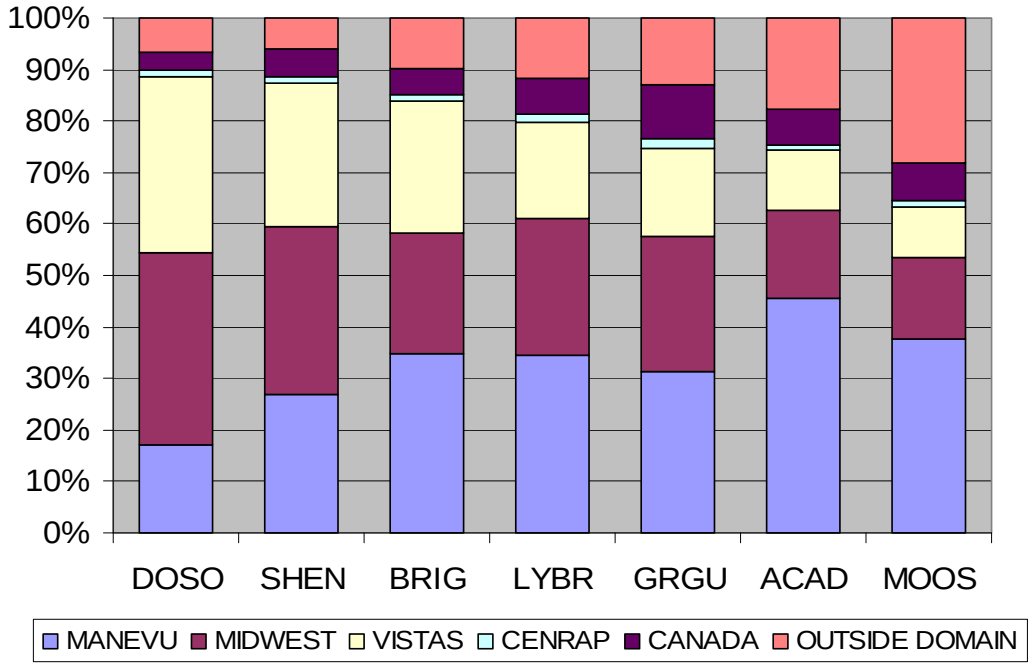

References

Byun, D.W., and Ching, J.K.S., *Science Algorithms of the EPA Models-3 Community Multiscale Air Quality (CMAQ) Modeling System*, EPA/600/R-99/030, March 1999.

Park, R. J., Jacob, D. J., Field, B. D., Yantosca, R. M., and Chin, M., *Natural and transboundary pollution influences on sulfate-nitrate-ammonium aerosols in the United States: implications for policy* , J. Geophys. Res., D15204, 10.1029/2003JD004473, 2004.

SAI, *User's Guide to the Regional Modeling System for Aerosols and Deposition (REMSAD), Version 7*, ICF Consulting/SAI, San Francisco, CA, 2002.

7. LAGRANGIAN DISPERSION MODELS

Dispersion models are commonly used to study the impacts of pollutant plumes or specific point source emissions on surrounding areas. The scale of these models has traditionally been limited to a few hundred kilometers because of a perceived lack of ability to accurately reproduce horizontal dispersion beyond these distances. Recent advances in the CALPUFF system (USEPA, 2006) — including enhancements to its horizontal diffusion and dispersion algorithms as well as the addition of chemical transformation parameterizations — have resulted in improved performance over much greater distances. In fact, the most recent proposed guidance for implementing the BART (Best Available Retrofit Technology) requirements of the Regional Haze Rule provide for the use of CALPUFF to analyze dispersion over distances exceeding 200 km as long as a detailed modeling protocol is included for approval by the appropriate reviewing authority (40 CFR Part 51, pg. 25194, May 5, 2004).

Appendix D provides specific information related to two CALPUFF platforms that have been developed for a large domain (see Figure 7-1) by the Vermont Department of Environmental Conservation (VT DEC) Air Pollution Control Branch and by the State of Maryland's Department of the Environment (MDE) and Department of Natural Resources (MDNR) with contract assistance provided by Environmental Resources Management (ERM). Appendix D contains detailed descriptions of the two platforms; the processing and evaluation of both MM5- and National Weather Service (NWS)-based meteorological data; the processing and evaluation of CEMS (Continuous Emissions Monitoring System)- and 2002 RPO-based emissions data; performance evaluations of

Figure 7-1. CALPUFF modeling domain utilized by MANE-VU

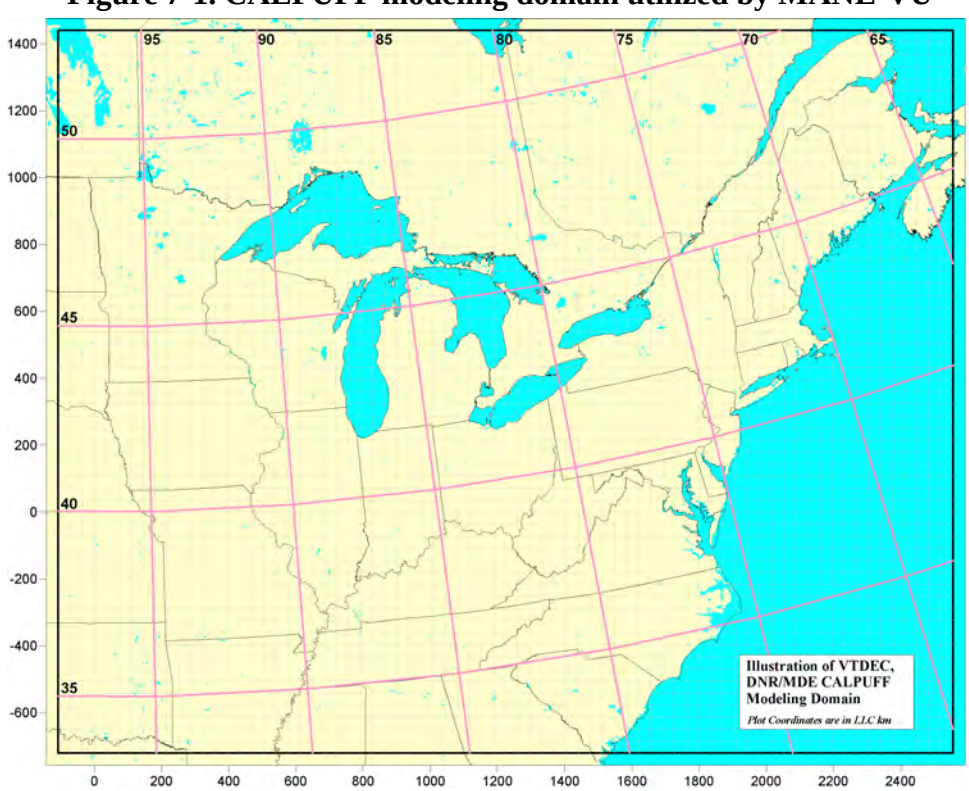

the overall modeling system; preliminary results of modeling to determine annual average and maximum 24-hour impact by individual unit and by state; and discussion of the future application of these platforms to the BART program. This chapter provides an overview of the two modeling platforms, a summary of initial results, and a brief analysis of the differences between the two platforms.

While CALPUFF will certainly play a role in helping MANE-VU assess potential visibility impacts for BART-eligible sources, the development of twin CALPUFF platforms utilizing both MM5-based and NWS-based meteorological drivers further expands the suite of analytical tools available for assessing contributions — at both the facility and state level — to downwind visibility impairment in the MANE-VU region.

7.1. Platform Overview

The VT DEC developed meteorological inputs for CALPUFF using observation-based inputs (i.e., rawinsonde and surface measurements) from the NWS and by applying CALMET. VT DEC also developed hourly emissions and exhaust flow data from the Acid Rain Program's CEMS data files for 869 large electric generating units (EGUs). These emissions data were utilized as inputs to CALPUFF, along with emissions data for four additional source sectors: non-EGU point sources, mobile (on-road), mobile (off-road), and general area sources. The emission inputs for these source sectors were derived from the 2002 RPO inventories.

The MDNR and MDE developed meteorological inputs for CALPUFF using MM5 data developed by the University of Maryland for the MANE-VU and Ozone Transport Commission SIP modeling work. The Maryland agencies utilized the CEMS data files developed by VT DEC, and independently developed emissions and source parameters for the other four source sectors based on the same inter-RPO 2002 inventories.

Both platforms were used to model the entire calendar year 2002. These simulations have been configured to provide estimates for both individual source impacts and cumulative state impacts and to allow for inter-platform comparisons. The modeling domain has been designed to be consistent with the other modeling systems described in this report (e.g., REMSAD, CMAQ), so that conclusions regarding the most significant sources of sulfate-related visibility impacts in MANE-VU can be compared. Consistency across a broad range of approaches will add credibility to the conclusions reached in the overall contribution assessment.

7.2. CALPUFF Modeling Results for Individual Sources

To explore differences between the two CALPUFF modeling platforms, each was used to create a ranked list of the 100 emissions sources that contribute most to ambient sulfate levels at each of several eastern Class I sites. Of the 100 top sources identified for the Brigantine Wilderness Area, 70 sources appeared on the lists generated by both platforms. At Acadia, Lye Brook, and Shenandoah, there was even more agreement between the model results, with both platforms identifying 78, 76, and 85 out of 100 of the same top sources for each of these sites, respectively. Figure 7-2 shows the correlation between estimated annual average impacts for the sources that were identified by both platforms as among the top 100 sulfate contributors. While the

NWS/rawindsonde-based meteorology consistently produced slightly lower estimates of impact than the MM5-based platform, the correlations are relatively robust, ranging from 0.89 at Brigantine to 0.93 at Lye Brook.

Overall, the CALPUFF modeling results to date demonstrate reasonably good comparability between the two platforms (as illustrated by Figure 7-2 and Table 7-1), but they also suggest a consistent pattern of under prediction for one platform relative to the other.

7.3. CALPUFF Modeling Results Overview

Table 7-1 provides further comparisons of the results of CALPUFF modeling utilizing the two different platforms described earlier in this chapter: VT DEC (NWS/rawinsonde-based meteorology) and Maryland (MM5-based meteorology).[35] The table summarizes annual average sulfate concentrations by source category for each of the two platforms relative to observed concentrations.

Table 7-1. CALPUFF Overall Modeling Summary

	Annual Average SO_4 Ion Concentration ($\mu g/m^3$)								
	NWS/Rawinsonde-based Meteorology				MM5-based Meteorology				Observed
	CEMS EGU	Non-CEMS Point	Area/Mobile	Total	CEMS EGU	Non-CEMS Point	Area/Mobile	Total	
Shenandoah	2.271	0.412	0.106	2.789	2.98	0.46	0.22	3.66	4.61
Brigantine	1.847	0.421	0.257	2.526	2.6	0.51	0.38	3.48	4.06
Acadia	0.965	0.385	0.218	1.569	1.42	0.42	0.28	2.13	1.86
Lye Brook	1.178	0.342	0.178	1.698	1.65	0.36	0.25	2.26	2.17

Generally, the NWS/rawinsonde platform predicts lower sulfate ion concentrations than the MM5 platform. On an annual average basis, the concentrations predicted using the MM5 platform are much closer to observed values than the concentrations predicted using the NWS/rawindsonde platform.

7.4. CALPUFF Results for Ranked State Sulfate Contributions

This section focuses on the ranked contribution of emissions from individual states to overall sulfate levels at specific receptor sites (additional results are summarized in a number of different ways in Appendix D). The rankings were calculated by summing impacts from EGUs included in the 2002 data base for each state. State contributions are then sorted by total annual impact. Predicted annual average sulfate ion concentrations from other source sectors were added to these data in Table 7-2(a-d) for both platforms. As in previous chapters, estimated contributions to receptor impact by state (using the results presented in Table 7-2) are depicted graphically in Figure 7-3 and Figure 7-4 for the observation-based and MM5-based platforms, respectively. States are ranked along the horizontal axis by averaging the individual results calculated for each state using the two CALPUFF platforms.

[35] The Maryland Department of the Environment is contributing toward this work through the Maryland Department of Natural Resources and their contractor ERM, Inc. who have developed the MM5-based meteorology and CALPUFF platform.

Figure 7-2. Correlation between MM5-based source contributions (Maryland/ERM) and NWS/rawindsonde-based source contributions (VT DEC) for common EGUs modeled at four receptor sites in or near MANE-VU

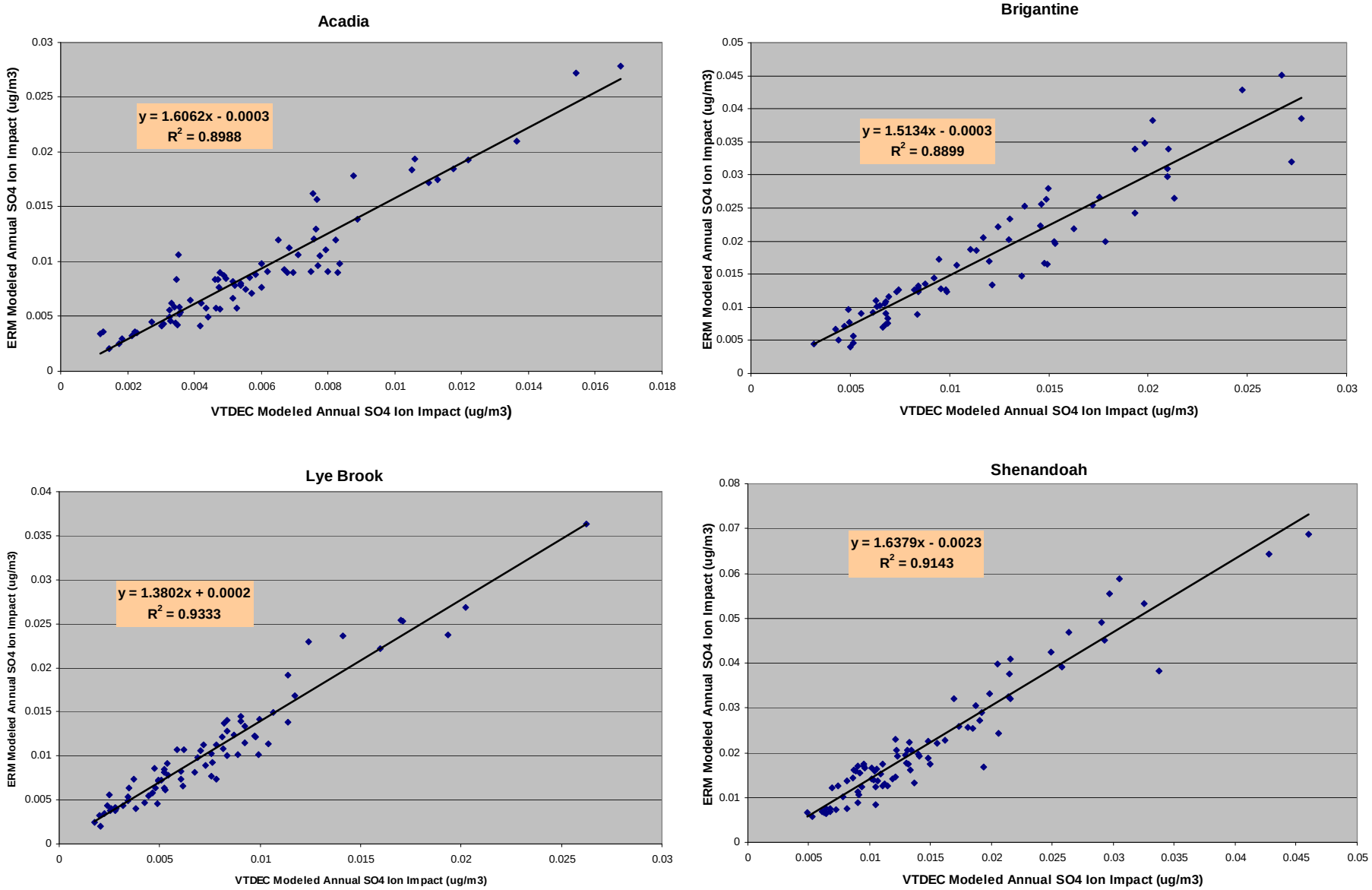

Table 7-2a. Sulfate Ion Impacts by State (Annual Average)
Acadia National Park

	NWS-based Meteorology (VT DEC) µg/m^3				MM5-based Meteorology (MDE/MDNR) µg/m^3			
STATE	**CEM PT**	**Non-CEM PT**	**Area/ Mobile**	**TOTAL PT**	**CEM PT**	**Non-CEM PT**	**Area/ Mobile**	**TOTAL**
AL(a)	0.0086	0.0013	0.0003	0.0102	0.0139	0.0009	0.0011	0.0159
AR(a)	0.0039	0	0	0.0039	0.0054	0.0020	0.0010	0.0083
CT	0.0041	0.0012	0.0085	0.0138	0.0074	0.0011	0.0072	0.0156
DC	0.0001	0.0001	0.0002	0.0004	6.9E-05	0.0001	0.0003	0.0005
DE	0.0087	0.002	0.0008	0.0115	0.0093	0.0109	0.0018	0.0219
GA(a)	0.0142	0.0008	0.0005	0.0155	0.0259	0.0009	0.0019	0.0287
IA	0.0097	0.0122	0.0001	0.0219	0.0149	0.0120	0.0030	0.0299
IL	0.0342	0.0157	0.0004	0.0504	0.0486	0.0172	0.0034	0.0693
IN	0.0758	0.0103	0.001	0.087	0.1089	0.0119	0.0099	0.1307
KS(a)	0.0081	0	0	0.0081	0.0137	0.0012	0.0010	0.0159
KY	0.0411	0.0054	0.0023	0.0487	0.0632	0.0038	0.0069	0.0740
MA	0.0653	0.0127	0.0579	0.136	0.0860	0.1544	0.0773	0.3176
MD	0.0398	0.0019	0.0034	0.0451	0.0780	0.0062	0.0040	0.0882
ME	0.0032	0.0243	0.0294	0.057	0.0030	0.0356	0.0236	0.0622
MI	0.0611	0.0083	0.0031	0.0726	0.0656	0.0095	0.0093	0.0844
MN	0.0089	0.0043	0.0005	0.0137	0.0107	0.0022	0.0023	0.0151
MO	0.014	0	0	0.014	0.0215	0.0115	0.0041	0.0371
MS(a)	0	0.0002	0.0002	0.0003	0	0.0002	0.0002	0.0004
NC	0.0342	0.0081	0.0014	0.0437	0.0554	0.0057	0.0019	0.0630
ND(a)					0	0.0009	0.0012	0.0021
NE(a)	0.0017	0	0	0.0017	0.0028	0	0.0009	0.0037
NH	0.0386	0.0022	0.0071	0.0479	0.0666	0.0020	0.0065	0.0750
NJ	0.013	0.0025	0.0076	0.0232	0.0187	0.0033	0.0133	0.0354
NY	0.0577	0.0118	0.0505	0.12	0.0736	0.0363	0.0578	0.1677
OH	0.1402	0.0081	0.0013	0.1496	0.2248	0.0457	0.0055	0.2759
OK(a)	0.0059	0	0	0.0059	0.0071	0.0015	0.0006	0.0092
PA	0.1383	0.0196	0.0126	0.1706	0.2354	0.0214	0.0156	0.2725
RI	0	0	0.0074	0.0074	5.9E-06	0.0007	0.0043	0.0050
SC	0.0092	0.003	0.001	0.0132	0.0134	0.0036	0.0012	0.0182
SD(a)	0.0009	0	0	0.0009	0.0012	2.8E-05	0.0009	0.0022
TN	0.0192	0.0045	0.0024	0.0261	0.0286	0.0076	0.0031	0.0393
TX(a)	0	0	0	0	1.1E-05	0	2.3E-05	3.5E-05
VA	0.0319	0.0082	0.0007	0.0407	0.0389	0.0081	0.0029	0.0499
VT	0	0.0004	0.0169	0.0173	4.0E-06	0.0004	0.0026	0.0030
WI	0.0152	0.0196	0.0005	0.0353	0.0254	0.0085	0.0019	0.0358
WV	0.0583	0.0053	0.0006	0.0642	0.0865	0.0086	0.0016	0.0966
Canada(b)	0	0.1914	0	0.1914				
Totals	**0.96511**	**0.3854**	**0.21832**	**1.5688**	**1.45**	**0.44**	**0.28**	**2.17**

Notes:

(a) Only sources in that portion of the state within the RPO modeling domain were modeled.

(b) 52 Canadian point sources > 250 tons/yr SO_2 emissions during 2002 (from Canadian NPRI).

Table 7-2b. Sulfate Ion Impacts by State (Annual Average) Brigantine Wilderness Area

	NWS-based Meteorology (VT DEC) µg/m^3				MM5-based Meteorology (MDE/MDNR) µg/m^3			
STATE	**CEM PT**	**Non-CEM PT**	**Area/ Mobile**	**TOTAL PT**	**CEM PT**	**Non-CEM PT**	**Area/ Mobile**	**TOTAL**
AL(a)	0.0317	0.0055	0.0011	0.0383	0.0304	0.0017	0.0020	0.0341
AR(a)	0.0047	0	0	0.0047	0.0088	0.0032	0.0017	0.0137
CT	0.0041	0.0013	0.0099	0.0153	0.0044	0.0009	0.0063	0.0116
DC	0.0009	0.0004	0.0008	0.0021	0.0012	0.0005	0.0013	0.0030
DE	0.0395	0.0111	0.0073	0.0579	0.0524	0.0549	0.0138	0.1211
GA(a)	0.0576	0.0044	0.0030	0.0649	0.0672	0.0024	0.0057	0.0753
IA	0.0156	0.0176	0.0001	0.0333	0.0152	0.0137	0.0032	0.0321
IL	0.0521	0.0192	0.0005	0.0719	0.0535	0.0190	0.0043	0.0768
IN	0.1165	0.0125	0.0011	0.1302	0.1632	0.0162	0.0128	0.1921
KS(a)	0.0113	0	0	0.0113	0.0107	0.0009	0.0008	0.0124
KY	0.0846	0.0098	0.0039	0.0982	0.1285	0.0076	0.0135	0.1496
MA	0.0240	0.0049	0.0191	0.0480	0.0234	0.0406	0.0168	0.0808
MD	0.1351	0.0073	0.0165	0.1589	0.2191	0.0228	0.0210	0.2630
ME	0.0004	0.0017	0.0016	0.0037	0.0002	0.0017	0.0011	0.0030
MI	0.0579	0.0077	0.0028	0.0685	0.0810	0.0110	0.0120	0.1040
MN	0.0120	0.0056	0.0007	0.0183	0.0114	0.0025	0.0027	0.0166
MO	0.0179	0	0	0.0179	0.0202	0.0108	0.0036	0.0346
MS(a)	0	0.0006	0.0003	0.0009	0	0.0006	0.0005	0.0012
NC	0.1414	0.0360	0.0060	0.1835	0.1609	0.0160	0.0054	0.1823
ND(a)					0	0.0011	0.0015	0.0026
NE(a)	0.0031	0	0	0.0031	0.0025	0	0.0009	0.0035
NH	0.0064	0.0004	0.0012	0.0080	0.0100	0.0003	0.0010	0.0113
NJ	0.0426	0.0081	0.0518	0.1024	0.0625	0.0124	0.0805	0.1553
NY	0.0658	0.0120	0.0719	0.1497	0.0810	0.0307	0.0779	0.1896
OH	0.2611	0.0130	0.0017	0.2757	0.4297	0.0836	0.0088	0.5221
OK(a)	0.0068	0	0	0.0068	0.0077	0.0014	0.0007	0.0098
PA	0.2538	0.0460	0.0339	0.3336	0.4407	0.0553	0.0461	0.5421
RI	0	0	0.0042	0.0042	2.1E-06	0.0003	0.0016	0.0019
SC	0.0362	0.0139	0.0042	0.0542	0.0341	0.0101	0.0032	0.0475
SD(a)	0.0011	0	0	0.0011	0.0012	3.4E-05	0.0012	0.0024
TN	0.0477	0.0138	0.0049	0.0664	0.0630	0.0188	0.0061	0.0879
TX(a)	0	0	0	0	2.5E-07	0	2.9E-05	3.0E-05
VA	0.1442	0.0447	0.0035	0.1924	0.1577	0.0331	0.0119	0.2027
VT	0	0.0002	0.0033	0.0035	1.5E-06	0.0001	0.0006	0.0008
WI	0.0216	0.0312	0.0007	0.0535	0.0315	0.0106	0.0026	0.0447
WV	0.1499	0.0118	0.0016	0.1633	0.2340	0.0202	0.0046	0.2588
Canada(b)	0	0.0807	0	0.0807				
Totals	**1.84732**	**0.42121**	**0.25746**	**2.526**	**2.61**	**0.51**	**0.38**	**3.49**

Notes:

(a) Only sources in that portion of the state within the RPO modeling domain were modeled.

(b) 52 Canadian point sources > 250 tons/yr SO_2 emissions during 2002 (from Canadian NPRI).

Table 7-2c. Sulfate Ion Impacts by State (Annual Average)
Lye Brook Wilderness Area

	NWS-based Meteorology (VT DEC) $\mu g/m^3$				MM5-based Meteorology (MDE/MDNR) $\mu g/m^3$			
STATE	**CEM PT**	**Non-CEM PT**	**Area/ Mobile**	**TOTAL PT**	**CEM PT**	**Non-CEM PT**	**Area/ Mobile**	**TOTAL**
AL(a)	0.0151	0.0023	0.0005	0.0179	0.0209	0.0013	0.0015	0.0238
AR(a)	0.0053	0	0	0.0053	0.0072	0.0029	0.0015	0.0116
CT	0.0015	0.0004	0.0038	0.0057	0.0024	0.0006	0.0045	0.0075
DC	0.0001	0.0002	0.0003	0.0005	7.9E-05	0.0002	0.0004	0.0006
DE	0.0045	0.0017	0.0007	0.0068	0.0076	0.0123	0.0020	0.0219
GA(a)	0.0270	0.0016	0.0011	0.0296	0.0351	0.0012	0.0029	0.0392
IA	0.0151	0.0175	0.0001	0.0326	0.0184	0.0158	0.0041	0.0383
IL	0.0473	0.0173	0.0005	0.0651	0.0550	0.0208	0.0047	0.0805
IN	0.1039	0.0120	0.0011	0.1170	0.1369	0.0148	0.0128	0.1645
KS(a)	0.0115	0	0	0.0115	0.0167	0.0016	0.0013	0.0195
KY	0.0647	0.0075	0.0031	0.0753	0.0820	0.0047	0.0099	0.0967
MA	0.0106	0.0040	0.0125	0.0270	0.0161	0.0291	0.0203	0.0655
MD	0.0452	0.0025	0.0040	0.0518	0.0686	0.0088	0.0052	0.0826
ME	0.0001	0.0020	0.0017	0.0038	0.0003	0.0024	0.0018	0.0044
MI	0.0841	0.0113	0.0041	0.0995	0.0798	0.0121	0.0120	0.1039
MN	0.0130	0.0062	0.0007	0.0200	0.0147	0.0031	0.0035	0.0213
MO	0.0191	0	0	0.0191	0.0253	0.0140	0.0052	0.0445
MS(a)	0	0.0004	0.0002	0.0006	0	0.0006	0.0004	0.0011
NC	0.0424	0.0088	0.0016	0.0528	0.0680	0.0058	0.0022	0.0760
ND(a)					0	0.0014	0.0020	0.0035
NE(a)	0.0027	0	0	0.0027	0.0032	0	0.0012	0.0044
NH	0.0072	0.0007	0.0020	0.0098	0.0137	0.0008	0.0023	0.0167
NJ	0.0071	0.0017	0.0051	0.0139	0.0128	0.0029	0.0115	0.0272
NY	0.0637	0.0289	0.0586	0.1511	0.0985	0.0613	0.0842	0.2440
OH	0.2108	0.0112	0.0016	0.2237	0.2963	0.0649	0.0078	0.3690
OK(a)	0.0086	0	0	0.0086	0.0097	0.0020	0.0009	0.0127
PA	0.1918	0.0255	0.0169	0.2342	0.3050	0.0288	0.0219	0.3558
RI	0	0	0.0013	0.0013	1.4E-06	0.0002	0.0010	0.0012
SC	0.0088	0.0037	0.0013	0.0138	0.0133	0.0040	0.0014	0.0187
SD(a)	0.0014	0	0	0.0014	0.0017	4.3E-05	0.0014	0.0031
TN	0.0281	0.0065	0.0032	0.0378	0.0407	0.0098	0.0042	0.0546
TX(a)	0	0	0	0	8.4E-06	0	3.2E-05	4.0E-05
VA	0.0295	0.0088	0.0008	0.0391	0.0454	0.0104	0.0037	0.0596
VT	0	0.0006	0.0499	0.0505	4.0E-06	0.0017	0.0083	0.0100
WI	0.0229	0.0293	0.0007	0.0529	0.0351	0.0116	0.0028	0.0495
WV	0.0852	0.0079	0.0009	0.0939	0.1232	0.0121	0.0023	0.1375
Canada(b)	0	0.1211	0	0.1211				
Totals	**1.1780**	**0.3416**	**0.1781**	**1.6977**	**1.65**	**0.36**	**0.25**	**2.27**

Notes:

(a) Only sources in that portion of the state within the RPO modeling domain were modeled.

(b) 52 Canadian point sources > 250 tons/yr SO_2 emissions during 2002 (from Canadian NPRI).

Table 7-2d. Sulfate Ion Impacts by State (Annual Average) Shenandoah National Park

	NWS-based Meteorology (VT DEC) µg/m^3				MM5-based Meteorology (MDE/MDNR) µg/m^3			
STATE	**CEM PT**	**Non-CEM PT**	**Area/ Mobile**	**TOTAL PT**	**CEM PT**	**Non-CEM PT**	**Area/ Mobile**	**TOTAL**
AL(a)	0.0521	0.0084	0.0018	0.0623	0.0504	0.0029	0.0034	0.0567
AR(a)	0.0074	0	0	0.0074	0.0087	0.0035	0.0019	0.0141
CT	0.0005	0.0002	0.0011	0.0018	0.0007	0.0001	0.0009	0.0017
DC	0.0004	0.0004	0.0008	0.0016	8.1E-05	0.0003	0.0009	0.0013
DE	0.0101	0.0029	0.0011	0.0141	0.0086	0.0136	0.0021	0.0243
GA(a)	0.0879	0.0056	0.0040	0.0975	0.0963	0.0032	0.0079	0.1073
IA	0.0192	0.0181	0.0001	0.0374	0.0152	0.0130	0.0036	0.0318
IL	0.0646	0.0222	0.0006	0.0874	0.0561	0.0189	0.0045	0.0794
IN	0.1782	0.0156	0.0015	0.1952	0.1907	0.0181	0.0155	0.2243
KS(a)	0.0137	0	0	0.0137	0.0091	0.0007	0.0006	0.0104
KY	0.1273	0.0135	0.0057	0.1465	0.1741	0.0106	0.0184	0.2031
MA	0.0036	0.0005	0.0020	0.0060	0.0029	0.0047	0.0023	0.0098
MD	0.1045	0.0116	0.0118	0.1280	0.1365	0.0373	0.0109	0.1847
ME	0	0.0004	0.0003	0.0007	2.8E-05	0.0003	0.0002	0.0006
MI	0.0830	0.0082	0.0036	0.0948	0.0860	0.0100	0.0125	0.1085
MN	0.0148	0.0055	0.0007	0.0210	0.0109	0.0023	0.0028	0.0160
MO	0.0255	0	0	0.0255	0.0180	0.0104	0.0034	0.0318
MS(a)	0	0.0009	0.0004	0.0013	0	0.0010	0.0007	0.0017
NC	0.1669	0.0251	0.0050	0.1970	0.2257	0.0148	0.0062	0.2467
ND(a)					0	0.0011	0.0016	0.0027
NE(a)	0.0038	0	0	0.0038	0.0023	0	0.0009	0.0032
NH	0.0010	0.0001	0.0002	0.0012	0.0013	5.3E-05	0.0002	0.0016
NJ	0.0102	0.0018	0.0046	0.0166	0.0119	0.0022	0.0071	0.0212
NY	0.0350	0.0027	0.0141	0.0519	0.0468	0.0141	0.0167	0.0776
OH	0.4678	0.0256	0.0027	0.4960	0.6483	0.1088	0.0114	0.7685
OK(a)	0.0080	0	0	0.0080	0.0081	0.0016	0.0009	0.0105
PA	0.2774	0.0354	0.0214	0.3342	0.4517	0.0318	0.0247	0.5082
RI	0	0	0.0004	0.0004	3.1E-07	2.9E-05	0.0002	0.0002
SC	0.0242	0.0117	0.0041	0.0401	0.0232	0.0093	0.0035	0.0359
SD(a)	0.0011	0	0	0.0011	0.0011	4.0E-05	0.0014	0.0025
TN	0.0781	0.0207	0.0073	0.1061	0.0929	0.0304	0.0086	0.1319
TX(a)	0	0	0	0	1.7E-07	0	3.2E-05	3.2E-05
VA	0.1102	0.0398	0.0047	0.1547	0.1124	0.0469	0.0263	0.1856
VT	0	0	0.0006	0.0007	3.6E-07	2.6E-05	0.0001	0.0002
WI	0.0259	0.0311	0.0007	0.0577	0.0289	0.0096	0.0026	0.0410
WV	0.2691	0.0259	0.0045	0.2995	0.4657	0.0402	0.0111	0.5170
Canada(b)	0	0.0781	0	0.0781				
Totals	**2.271**	**0.412**	**0.106**	**2.789**	**2.98**	**0.46**	**0.22**	**3.66**

Notes:

(a) Only sources in that portion of the state within the RPO modeling domain were modeled.

(b) 52 Canadian point sources > 250 tons/yr SO_2 emissions during 2002 (from Canadian NPRI).

Figure 7-3a. Ranked state percent sulfate contributions to Northeast Class I receptors based on observation-based (VT) CALPUFF results

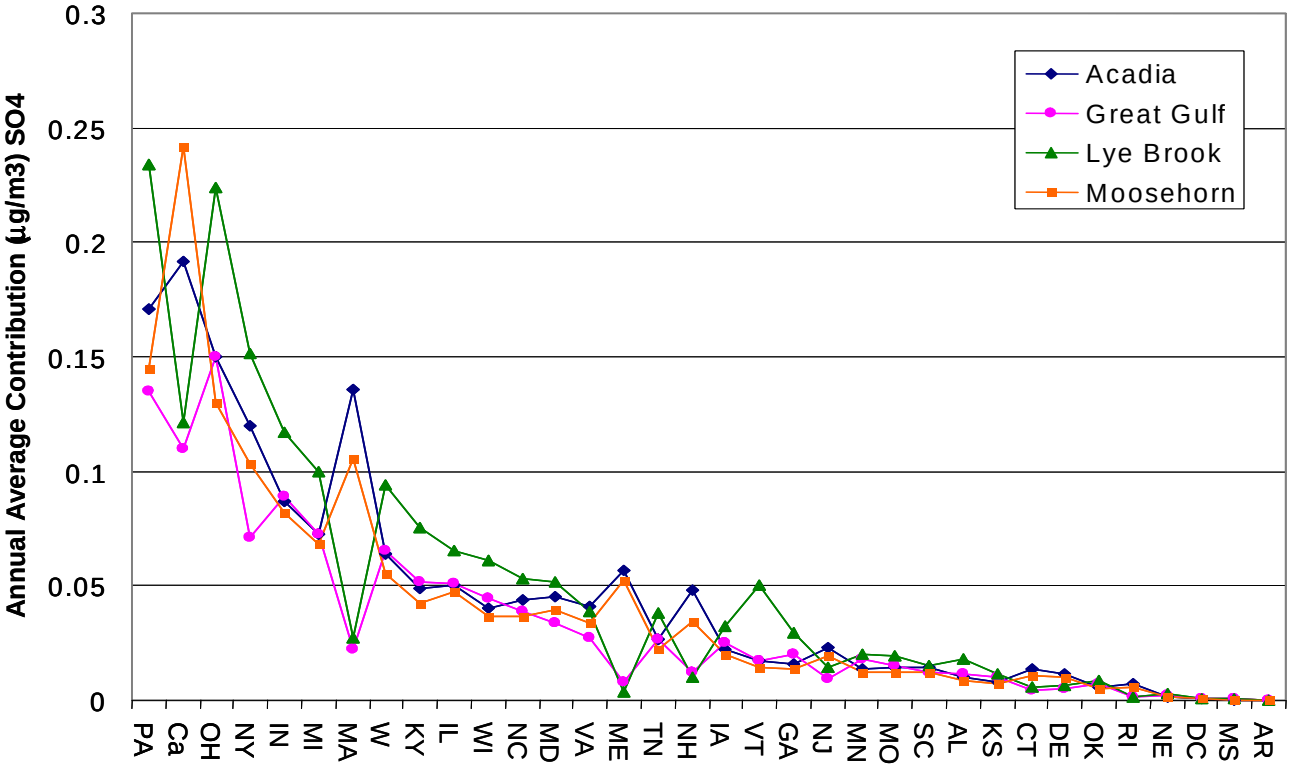

Figure 7-3b. Ranked state percent sulfate contributions to Mid-Atlantic Class I receptors based on observation-based (VT) CALPUFF results

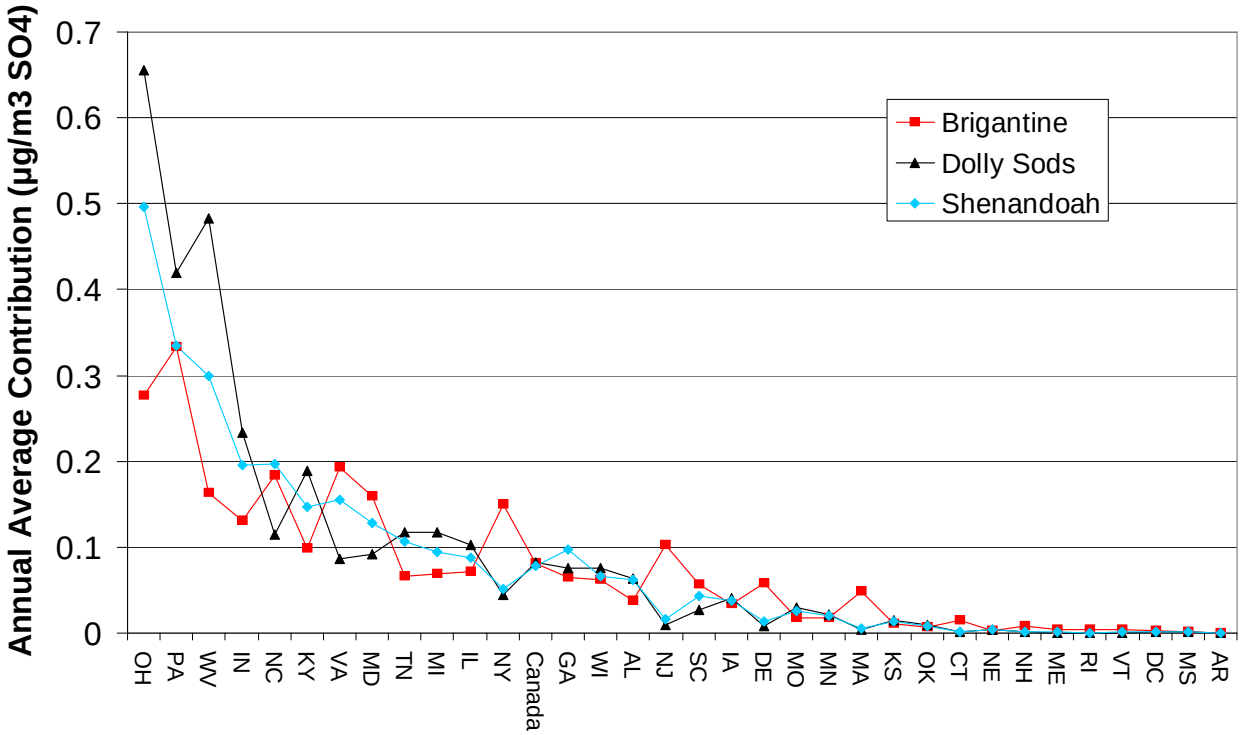

Figure 7-4a. Ranked state percent sulfate contributions to Northeast Class I receptors based on MM5-based (MD) CALPUFF results

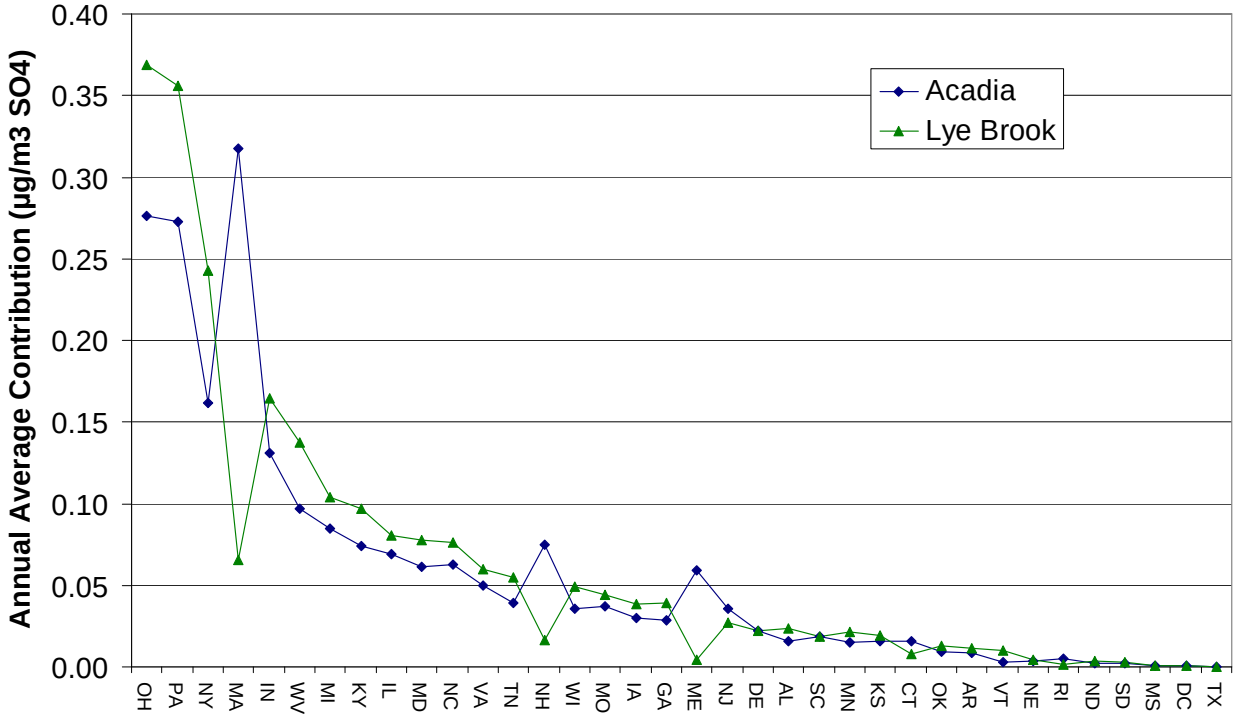

Figure 7-4b. Ranked state percent sulfate contributions to Mid-Atlantic Class I receptors based on MM5-based (MD) CALPUFF results

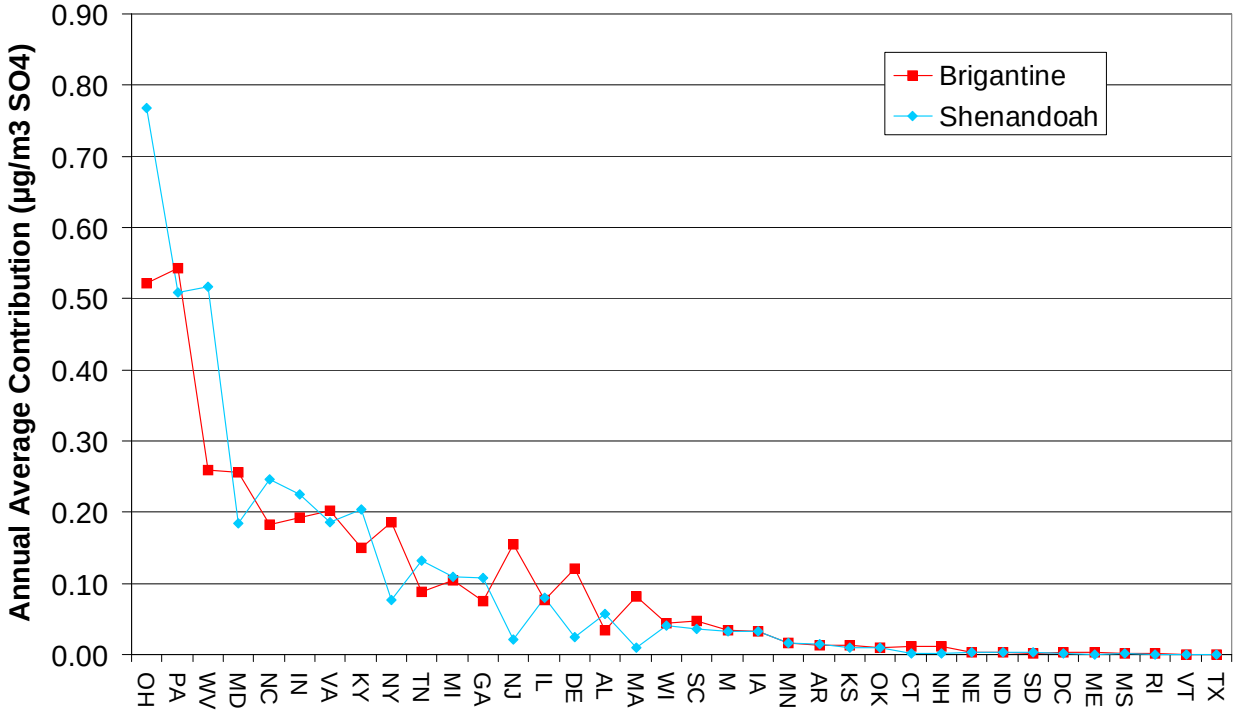

7.5. Future work and potential uses of CALPUFF results for BART determinations

Modeling efforts to date have provided a solid basis for contributing to a weight-of-evidence assessment of state contributions. In addition, the two CALPUFF platforms can be used to evaluate the relative contributions to fine PM and visibility impacts of individual sources in the MANE-VU region. It is anticipated that MANE-VU will provide all states with a consistent set of modeling results from each of these platforms to serve as a preliminary basis for BART visibility determinations and states will have several options with regard to how these results are used:

- States may accept the MANE-VU modeling as an adequate basis for determining whether BART controls at a facility are justified by its contribution to visibility degradation.

- States may conduct additional modeling on their own to determine whether BART controls at a facility are justified by its contribution to visibility degradation.

- States may require a source to conduct additional modeling to determine whether BART controls at a facility are justified by its contribution to visibility degradation.

These options and the use of modeling results for BART determinations are discussed in more detail in the *MANE-VU BART Resource Book* (NESCAUM, 2006), and the reader is referred to that resource for additional information.

References

NESCAUM, *BART Resource Guide*, Northeast States for Coordinated Air Use Management, 2006.

USEPA, CALPUFF Modeling System, Available at: http://www.epa.gov/ttn/scram, 2006.

8. SYNTHESIS OF RESULTS USING DIFFERENT SOURCE ASSESSMENT TECHNIQUES

By synthesizing results from a variety of data sources and analysis techniques MANE-VU has taken a first step toward identifying sources of visibility impairment in the Northeast generally, and toward understanding the role of transported sulfate in particular. The variety of approach and complexity of analytical tools utilized for this purpose provides numerous metrics and means of comparison into how SO_2 emissions are chemically transformed, transported and combined with various local constituents of fine particle pollution in the MANE-VU region. Beyond reviewing these results, additional sections of this chapter describe opportunities for further synthesizing the available data to solidify a weight-of-evidence approach to implementing the contribution assessment and pollution apportionment requirements of the Haze Rule

8.1. Ranked Contribution

Chapter 4 of this report describes two crude methods of ranking state contributions based on the ratio of source emissions to source-receptor distance as well as the gridded product of emissions and upwind residence time probability. Chapter 5 describes the qualitative evidence available from several different trajectory-based techniques and source apportionment studies. These include source region comparisons, source profile examinations, and the development of other techniques and metrics to support the more quantitative ranking techniques. Chapter 6 describes results obtained using Eulerian grid models such as the Regulatory Modeling System for Aerosols and Deposition (REMSAD) and the Community Multi-scale Air Quality (CMAQ) model. Ultimately these types of models are likely to yield the most definitive assessments of contribution from different sources. Chapter 7 explores the use of lagrangian puff dispersion models such as CALPUFF for estimating source contributions and compares two related but distinct versions of the CALPUFF modeling system that demonstrate the sensitivity of this tool to emissions and meteorology inputs.

In Table 8-1 through Table 8-5 (and graphically in Figure 8-1), we have normalized the results obtained using five techniques for assessing state contribution by calculating the percentage contribution and plotted them on a common graph. The figure shows substantial consistency across a variety of independent analyses using techniques that are themselves based on the application of disparate chemical, meteorological and physical principles. Together, these findings create a strong weight-of-evidence case for identifying the most significant contributors to visibility impairment in MANE-VU Class I areas.

In Figure 8-1, several features of the normalized results bear notice. First, we note that the apparent perfect agreement among the techniques for the “other” contribution that represents all emissions from outside the domain of study is a result of having substituted the REMSAD calculated “other” contribution for all of the other methods. REMSAD is the only method that has a means of developing a comprehensive estimate of the total out-of-domain contribution because the boundary condition used was derived from a global model run using global SO_2 emissions estimates. It is also worth noting how high the “other,” or out-of-domain, contribution is to observed sulfate at

Acadia National Park. This is not surprising given how close Acadia is to the domain boundaries on both the northern and eastern edge. There may be some recirculation of in-domain SO_2 emissions that leave the modeling domain and re-enter through the dynamic boundary condition, but lose their tag in the process.

It is also worth noting the differences between the methods for certain states and Canada, such as Massachusetts and Maine in the case of Acadia, Maryland and Canada for Brigantine, Canada for Lye Brook, and Ohio and West Virginia for Shenandoah. Those states and Canada that are directly upwind a large fraction of the time, either because they are very large geographically or because they are very nearby, are likely to be treated differently by the percent-time-upwind method relative to the other methods. In addition, the CALPUFF models appear to underestimate the contribution from Canada relative to other methods. This is likely to result from an incomplete characterization of the total SO_2 inventory for Canada relative to other methods that are based on the entire MANE-VU Canadian inventory.

Table 8-1. Annual Average Sulfate Impact from REMSAD (%)

RPO	STATE	ACADIA	BRIGANTINE	DOLLY SODS	GREAT GULF	LYE BROOK	MOOSEHORN	SHENANDOAH
CANADA		**8.69**	**7.11**	**3.90**	**14.84**	**12.43**	**7.85**	**4.75**
CENRAP		**0.88**	**1.12**	**1.58**	**1.65**	**1.67**	**0.82**	**1.48**
MANE-VU		**36.17**	**34.83**	**14.81**	**27.83**	**31.78**	**30.08**	**20.59**
MANE-VU	Connecticut	0.76	0.53	0.04	0.48	0.55	0.56	0.08
	Delaware	0.96	3.20	0.30	0.63	0.93	0.71	0.61
	District of Columbia	0.01	0.04	0.01	0.01	0.02	0.01	0.04
	Maine	6.54	0.16	0.01	2.33	0.31	8.01	0.02
	Maryland	2.20	4.98	2.39	1.92	2.66	1.60	4.84
	Massachusetts	10.11	2.73	0.18	3.11	2.45	6.78	0.35
	New Hampshire	2.25	0.60	0.04	3.95	1.68	1.74	0.08
	New Jersey	1.40	4.04	0.27	0.89	1.44	1.03	0.48
	New York	4.74	5.57	1.32	5.68	9.00	3.83	2.03
	Pennsylvania	6.81	12.84	10.23	8.30	11.72	5.53	12.05
	Rhode Island	0.28	0.10	0.01	0.11	0.06	0.19	0.01
	Vermont	0.13	0.06	0.00	0.41	0.95	0.09	0.01
MIDWEST		**11.98**	**18.16**	**30.26**	**20.10**	**21.48**	**10.40**	**26.84**
MIDWEST	Illinois	1.37	1.82	2.56	2.52	2.42	1.30	2.47
	Indiana	2.13	3.29	5.40	3.94	3.93	2.02	5.23
	Michigan	2.02	2.77	3.24	3.88	3.67	1.74	3.20
	Ohio	5.62	9.11	17.98	8.33	9.96	4.62	14.87
	Wisconsin	0.85	1.16	1.08	1.42	1.49	0.72	1.07
VISTAS		**8.49**	**21.99**	**36.75**	**12.04**	**13.65**	**6.69**	**33.86**
VISTAS	Alabama	0.32	1.07	2.13	0.65	0.81	0.25	1.77
	Georgia	0.67	2.32	3.71	1.27	1.31	0.56	3.47
	Kentucky	1.17	2.22	4.89	1.99	2.22	0.98	4.34
	Mississippi	0.01	0.04	0.08	0.03	0.04	0.01	0.07
	North Carolina	1.45	4.19	4.29	1.88	1.89	1.14	4.78
	South Carolina	0.43	1.69	1.04	0.64	0.56	0.36	1.30
	Tennessee	0.61	1.56	3.41	1.11	1.23	0.50	2.73
	Virginia	1.48	4.30	2.82	1.52	1.95	1.13	6.20
	West Virginia	2.35	4.59	14.38	2.96	3.64	1.75	9.19
OTHER		**33.79**	**16.78**	**12.70**	**23.54**	**18.99**	**44.17**	**12.48**
TOTAL ($\mu g/m^3$)		**2.026**	**3.444**	**3.867**	**1.780**	**2.137**	**1.767**	**3.919**

Table 8-2. Annual Average Sulfate Impact from Q/D (%)

RPO	STATE	ACADIA	BRIGANTINE	DOLLY SODS	GREAT GULF	LYE BROOK	MOOSEHORN	SHENANDOAH
CANADA		**11.91**	**6.01**	**0.00**	**8.97**	**12.00**	**18.77**	**6.76**
CENRAP		**1.74**	**1.64**	**1.59**	**2.33**	**1.99**	**1.35**	**1.72**
CENRAP	Arkansas	0.13	0.15	0.13	0.08	0.17	0.09	0.26
	Iowa	0.29	0.19	0.24	0.40	0.32	0.24	0.24
	Louisiana	0.02	0.03	0.02	0.02	0.03	0.02	0.04
	Minnesota	0.22	0.13	0.16	0.30	0.24	0.13	0.19
	Missouri	1.08	1.15	1.03	1.53	1.23	0.87	1.00
MANE-VU		**20.13**	**32.53**	**20.10**	**21.48**	**25.69**	**12.84**	**24.50**
MANE-VU	Connecticut	0.34	0.33	0.11	0.74	0.38	0.21	0.31
	Delaware	0.59	3.01	0.46	0.51	0.67	0.36	1.07
	District of Columbia	0.01	0.05	0.02	0.01	0.02	0.01	0.09
	Maine	1.74	0.15	0.08	0.71	0.15	1.13	0.15
	Maryland	1.83	7.26	3.86	0.43	2.67	1.27	5.27
	Massachusetts	2.89	0.95	0.46	4.61	1.06	1.33	1.22
	New Hampshire	1.07	0.30	0.14	0.42	0.08	0.60	0.18
	New Jersey	0.76	4.22	0.43	3.11	0.75	0.48	1.82
	New York	4.02	4.61	1.93	3.67	6.71	2.83	3.30
	Pennsylvania	6.64	11.57	12.58	6.62	13.07	4.50	11.00
	Rhode Island	0.12	0.05	0.02	0.08	0.04	0.06	0.06
	Vermont	0.10	0.03	0.02	0.57	0.10	0.07	0.04
MIDWEST		**16.99**	**17.48**	**26.30**	**25.38**	**22.84**	**12.49**	**22.46**
MIDWEST	Illinois	2.53	2.16	2.60	3.64	2.98	2.11	2.61
	Indiana	3.94	4.24	5.17	6.01	5.01	2.91	4.50
	Michigan	2.69	1.95	2.46	4.08	3.50	2.16	2.49
	Ohio	6.63	8.34	15.06	9.94	9.98	4.51	11.85
	Wisconsin	1.19	0.79	1.00	1.71	1.38	0.80	1.01
VISTAS		**15.44**	**25.55**	**39.32**	**18.30**	**18.48**	**10.39**	**32.08**
VISTAS	Alabama	1.24	1.69	1.66	1.45	1.60	0.91	1.65
	Georgia	2.36	3.28	3.18	2.62	2.82	1.63	3.30
	Kentucky	2.07	3.36	3.99	3.18	2.79	1.50	3.54
	Mississippi	0.19	0.24	0.22	0.22	0.24	0.14	0.37
	North Carolina	2.27	4.16	9.03	2.59	2.69	1.44	6.60
	South Carolina	1.29	1.62	0.95	1.14	0.94	0.70	1.69
	Tennessee	1.45	2.14	2.49	1.74	1.92	1.06	2.40
	Virginia	1.93	4.36	2.49	1.97	1.78	1.12	4.25
	West Virginia	2.64	4.71	15.33	3.39	3.71	1.88	8.27
OTHER[36]		**33.79**	**16.78**	**12.70**	**23.54**	**18.99**	**44.17**	**12.48**
TOTAL ($\mu g/m^3$)		**1.920**	**2.740**	**3.455**	**1.305**	**1.858**	**1.977**	**3.417**

[36] OTHER is % from REMSAD result; Florida is considered within OTHER

Table 8-3. Annual Average Sulfate Impact from CALPUFF (NWS Observations) (%)

RPO	STATE	ACADIA	BRIGANTINE	DOLLY SODS	GREAT GULF	LYE BROOK	MOOSEHORN	SHENANDOAH
CANADA		**8.07**	**2.65**	**2.30**	**7.22**	**5.77**	**9.45**	**2.45**
CENRAP		**2.76**	**2.98**	**3.34**	**5.06**	**4.50**	**2.30**	**3.42**
CENRAP	Iowa	0.93	1.09	1.13	1.65	1.55	0.80	1.17
	Kansas	0.34	0.37	0.41	0.64	0.55	0.28	0.43
	Louisiana	0.00	0.00	0.00	0.00	0.00	0.00	0.00
	Minnesota	0.58	0.60	0.62	1.16	0.95	0.49	0.65
	Missouri	0.59	0.59	0.81	1.00	0.91	0.49	0.80
	Nebraska	0.07	0.10	0.11	0.14	0.13	0.06	0.12
	Oklahoma	0.25	0.22	0.26	0.47	0.41	0.20	0.25
MANE-VU		**27.41**	**29.17**	**16.21**	**20.91**	**26.52**	**21.11**	**17.47**
MANE-VU	Connecticut	0.58	0.50	0.03	0.26	0.27	0.41	0.06
	Delaware	0.48	1.90	0.21	0.31	0.32	0.38	0.44
	District of Columbia	0.02	0.07	0.02	0.03	0.02	0.02	0.05
	Maine	2.40	0.12	0.01	0.53	0.18	2.04	0.02
	Maryland	1.90	5.22	2.54	2.19	2.47	1.55	4.01
	Massachusetts	5.73	1.58	0.12	1.44	1.29	4.13	0.19
	New Hampshire	2.02	0.26	0.02	0.79	0.47	1.36	0.04
	New Jersey	0.98	3.37	0.28	0.63	0.67	0.75	0.52
	New York	5.06	4.92	1.24	4.67	7.20	4.03	1.63
	Pennsylvania	7.19	10.97	11.71	8.86	11.16	5.65	10.48
	Rhode Island	0.31	0.14	0.01	0.08	0.06	0.22	0.01
	Vermont	0.73	0.12	0.01	1.13	2.41	0.56	0.02
MIDWEST		**16.85**	**19.99**	**33.09**	**26.68**	**26.98**	**14.21**	**29.46**
MIDWEST	Illinois	2.12	2.37	2.86	3.36	3.11	1.84	2.74
	Indiana	3.67	4.28	6.52	5.83	5.57	3.19	6.11
	Michigan	3.06	2.25	3.28	4.74	4.74	2.67	2.97
	Ohio	6.31	9.07	18.33	9.82	10.66	5.07	15.55
	Wisconsin	1.69	2.03	2.10	2.93	2.90	1.44	2.09
VISTAS		**11.12**	**28.43**	**32.35**	**16.59**	**17.24**	**8.76**	**34.72**
VISTAS	Alabama	0.43	1.26	1.77	0.77	0.85	0.32	1.96
	Georgia	0.65	2.13	2.12	1.30	1.41	0.52	3.06
	Kentucky	2.05	3.23	5.29	3.39	3.59	1.64	4.59
	Mississippi	0.01	0.03	0.04	0.03	0.03	0.01	0.04
	North Carolina	1.84	6.03	3.20	2.52	2.51	1.42	6.18
	South Carolina	0.61	1.87	0.75	0.80	0.71	0.49	1.33
	Tennessee	1.10	2.19	3.27	1.72	1.80	0.86	3.33
	Virginia	1.72	6.33	2.42	1.80	1.86	1.32	4.85
	West Virginia	2.71	5.37	13.49	4.26	4.48	2.17	9.39
OTHER[36]		**33.79**	**16.78**	**12.70**	**23.54**	**18.99**	**44.17**	**12.48**
TOTAL ($\mu g/m^3$)		**1.571**	**2.533**	**3.125**	**1.167**	**1.701**	**1.429**	**2.793**

Table 8-4. Annual Average Sulfate Impact from CALPUFF (MM5) (%)

RPO	STATE	ACADIA	BRIGANTINE	DOLLY SODS	GREAT GULF	LYE BROOK	MOOSEHORN	SHENANDOAH
CANADA		**8.05**	**2.65**			**5.76**		**2.46**
CENRAP		**3.26**	**2.85**			**5.08**		**2.74**
CENRAP	Arkansas	0.23	0.32			0.39		0.33
	Iowa	0.82	0.75			1.28		0.74
	Kansas	0.43	0.29			0.65		0.24
	Louisiana							
	Minnesota	0.41	0.39			0.71		0.37
	Missouri	1.01	0.80			1.48		0.74
	Nebraska	0.10	0.08			0.15		0.07
	Oklahoma	0.25	0.23			0.42		0.24
	Texas	0.00	0.00			0.00		0.00
MANE-VU		**28.09**	**31.83**			**27.69**		**19.31**
MANE-VU	Connecticut	0.43	0.27			0.25		0.04
	Delaware	0.01	0.07			0.02		0.03
	District of Columbia	0.60	2.81			0.73		0.57
	Maine	1.62	0.06			0.14		0.01
	Maryland	1.68	5.95			2.59		4.27
	Massachusetts	8.67	1.87			2.18		0.23
	New Hampshire	2.05	0.26			0.56		0.04
	New Jersey	0.97	3.60			0.91		0.49
	New York	4.41	4.30			8.08		1.79
	Pennsylvania	7.44	12.57			11.86		11.83
	Rhode Island	0.14	0.04			0.04		0.00
	Vermont	0.08	0.02			0.33		0.00
MIDWEST		**16.28**	**21.79**			**25.58**		**28.43**
MIDWEST	Illinois	1.89	1.78			2.68		1.85
	Indiana	3.57	4.46			5.48		5.22
	Michigan	2.30	2.41			3.47		2.53
	Ohio	7.53	12.11			12.30		17.88
	Wisconsin	0.98	1.04			1.65		0.95
VISTAS		**10.53**	**24.10**			**16.90**		**34.57**
VISTAS	Alabama	0.43	0.79			0.79		1.32
	Georgia	0.78	1.74			1.30		2.50
	Kentucky	2.02	3.47			3.22		4.73
	Mississippi	0.01	0.03			0.04		0.04
	North Carolina	1.72	4.23			2.53		5.74
	South Carolina	0.50	1.10			0.62		0.84
	Tennessee	1.07	2.04			1.82		3.07
	Virginia	1.36	4.70			1.99		4.32
	West Virginia	2.64	6.00			4.58		12.03
OTHER[36]		**33.79**	**16.78**	**12.70**	**23.54**	**18.99**	**44.17**	**12.48**
TOTAL ($\mu g/m^3$)		**2.424**	**3.589**			**2.430**		**3.761**

Table 8-5. Annual Average Sulfate Impact from percent time upwind method (%)

RPO	STATE	ACADIA	BRIGANTINE	DOLLY SODS	GREAT GULF	LYE BROOK	MOOSEHORN	SHENANDOAH
CANADA		**15.24**	**6.70**		**19.29**	**15.91**	**13.45**	**4.33**
CENRAP		**1.89**	**1.77**		**1.73**	**1.66**	**1.52**	**1.72**
CENRAP	Arkansas	0.12	0.24		0.15	0.15	0.15	0.20
	Iowa	0.38	0.27		0.27	0.28	0.28	0.25
	Kansas	0.00	0.00		0.00	0.00	0.00	0.00
	Louisiana	0.04	0.08		0.06	0.04	0.04	0.09
	Minnesota	0.56	0.33		0.38	0.44	0.44	0.22
	Missouri	0.80	0.85		0.87	0.75	0.62	0.95
	Texas	0.00	0.00		0.00	0.00	0.00	0.00
MANE-VU		**18.33**	**25.83**		**20.64**	**25.38**	**15.23**	**11.38**
MANE-VU	Connecticut	0.51	0.27		0.52	0.59	0.40	0.10
	Delaware	0.30	1.36		0.34	0.42	0.28	0.24
	District of Columbia	0.12	0.29		0.11	0.14	0.12	0.24
	Maine	1.49	0.08		0.68	0.26	1.53	0.05
	Maryland	1.32	3.06		1.31	1.31	0.96	2.29
	Massachusetts	1.10	0.33		0.86	0.81	0.90	0.12
	New Hampshire	1.21	0.17		1.48	0.72	0.77	0.06
	New Jersey	1.02	6.01		0.99	1.39	0.78	0.49
	New York	4.80	3.49		6.80	9.08	4.23	1.44
	Pennsylvania	6.21	10.71		7.10	10.36	5.07	6.33
	Rhode Island	0.11	0.05		0.08	0.08	0.09	0.02
	Vermont	0.14	0.03		0.37	0.23	0.10	0.01
MIDWEST		**17.35**	**19.55**		**20.67**	**21.63**	**15.56**	**22.03**
MIDWEST	Illinois	3.79	3.47		3.31	3.74	3.22	3.76
	Indiana	3.37	4.36		4.33	4.13	3.21	5.08
	Michigan	2.73	2.07		3.03	3.27	2.34	1.80
	Ohio	6.10	8.65		8.73	9.23	5.77	10.64
	Wisconsin	1.36	1.00		1.28	1.25	1.02	0.76
VISTAS		**13.40**	**29.37**		**14.14**	**16.43**	**10.07**	**48.06**
VISTAS	Alabama	0.72	1.32		0.63	0.71	0.39	2.14
	Georgia	1.40	3.21		1.06	1.54	0.72	4.73
	Kentucky	2.65	4.71		3.59	3.83	2.31	7.82
	Mississippi	0.04	0.10		0.06	0.06	0.03	0.12
	North Carolina	1.29	4.35		0.92	0.99	1.18	6.11
	South Carolina	0.72	1.64		0.42	0.41	0.44	1.62
	Tennessee	1.05	1.91		1.04	1.16	0.86	3.67
	Virginia	1.80	4.83		1.48	1.67	1.32	5.45
	West Virginia	3.74	7.31		4.94	6.05	2.81	16.39
OTHER[36]		**33.79**	**16.78**	**12.70**	**23.54**	**18.99**	**44.17**	**12.48**

MANE-VU will continue to explore these differences, but it remains encouraging that the use of different platforms and approaches results in more agreement across the various techniques than difference. With the few, specific exceptions mentioned above, it is relatively easy — using the normalized results from multiple techniques shown in Figure 8-1(a-d) — to identify those states that have the largest influence on sulfate levels at each Class I site. MANE-VU believes that this information can provide a solid basis for initiating consultation and planning efforts between upwind and downwind states and RPOs.

Figure 8-1(a-d). Comparison of normalized (percent contribution) results using different techniques for ranking state contributions to sulfate levels at the MANE-VU Class I sites (a) Acadia National Park, ME, (b) Brigantine Wilderness Area, NJ, (c)Lye Brook Wilderness Area, VT, and (d) Shenandoah National Park, VA.

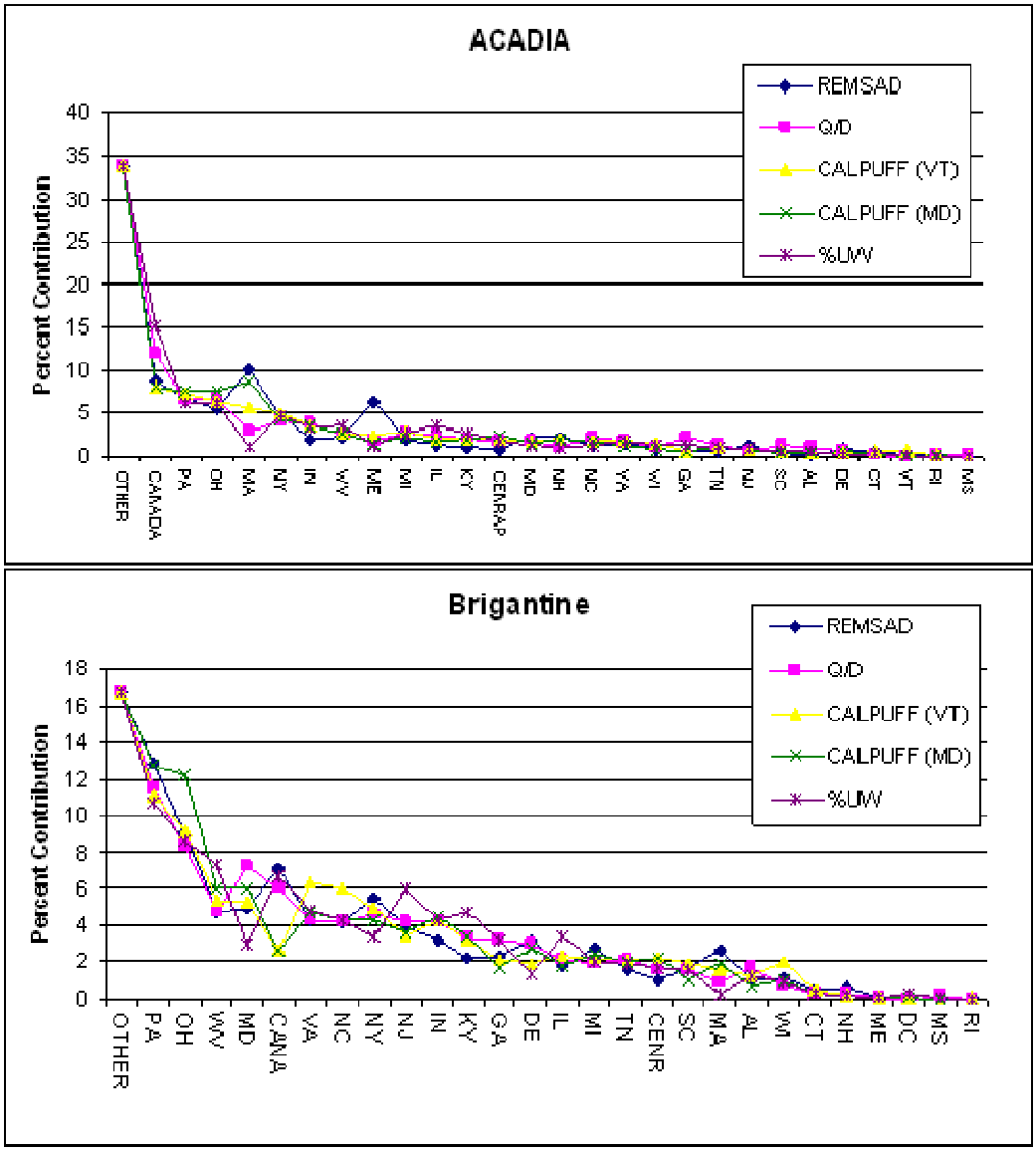

Figure 8-1(a-d). Continued

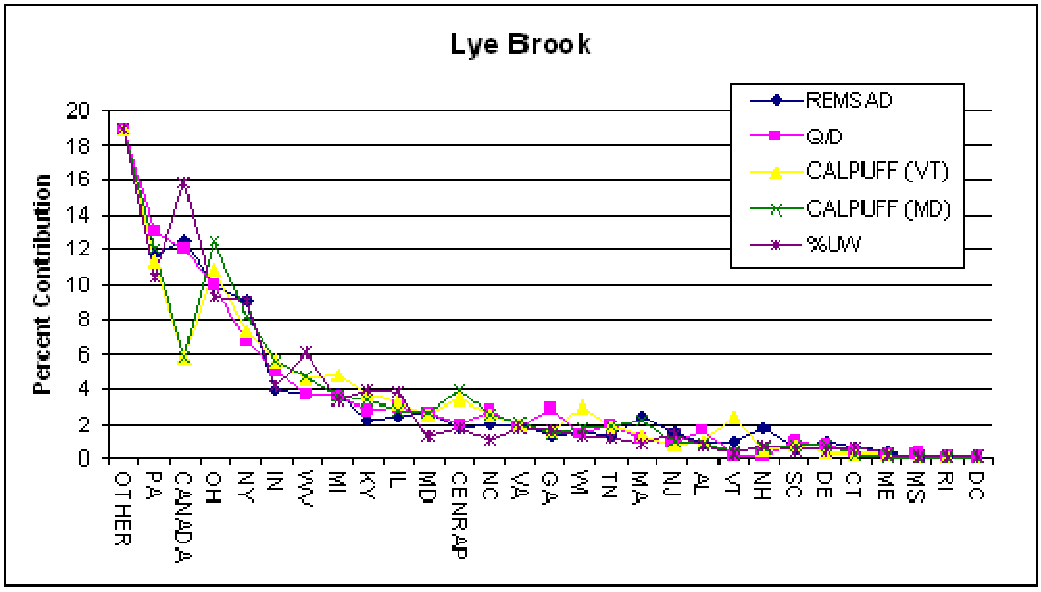

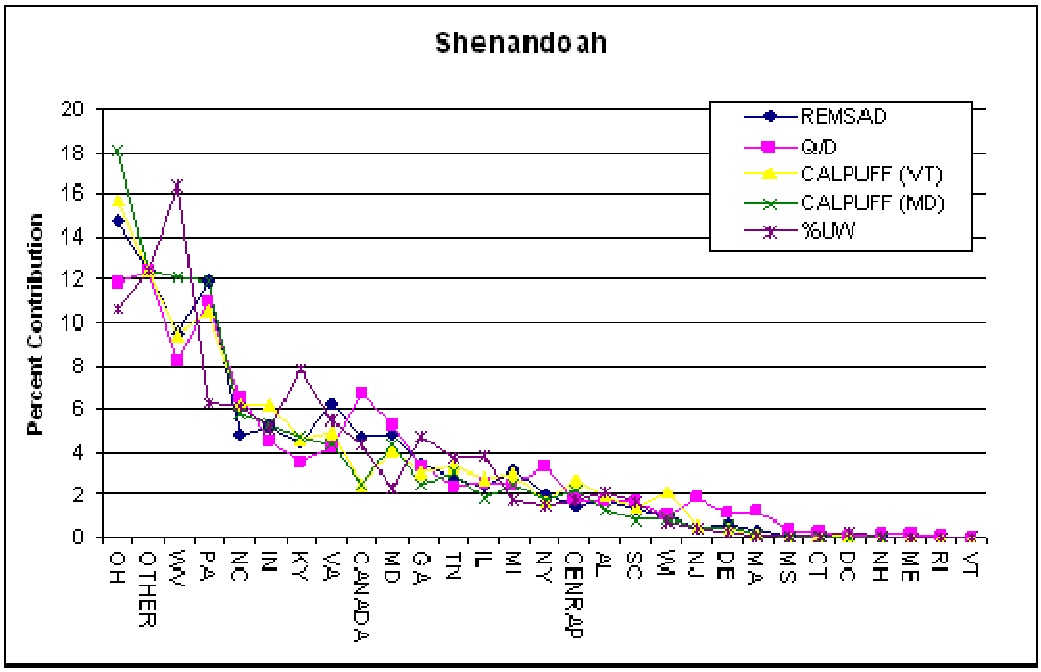

An alternative means of displaying the above results is in Table 8-6, which shows the individual state rankings produced by different assessment techniques for Acadia National Park, Maine. In the left-side column of Table 8-6, states are colored according to their average ranking across the different assessment methods. Those states that are ranked in the top five on average, across all techniques are colored red, while states ranked in the top six through ten are colored magenta, and so on for each group of five going down the left-side column. Through this color scheme, one can see how the states' average ranking compares to their rankings under each individual assessment method given in the other columns of the table. The fact that all techniques tend to come to

consistent conclusions about which states are top contributors provides some confidence that the source regions with the most influence on sulfate levels at MANE-VU Class I sites can be correctly identified. Note that the CENRAP states and several other states along the border of the analysis domain represent only partial state contributions.

Table 8-6. Ranked Contributing States to Acadia Sulfate

Average	REMSAD	Q/d	CALPUFF (VT)	CALPUFF (MD)	E x RTP
CANADA	MA	CANADA	CANADA	MA	CANADA
PA	CANADA	PA	PA	CANADA	PA
OH	PA	OH	OH	OH	OH
MA	ME	NY	MA	PA	NY
NY	OH	IN	NY	NY	IL
IN	NY	MA	IN	IN	WV
WV	WV	MI	MI	WV	IN
ME	NH	WV	WV	CENRAP	MI
MI	MD	IL	ME	MI	KY
IL	IN	GA	IL	NH	CENRAP
KY	MI	NC	CENRAP	KY	VA
CENRAP	VA	KY	KY	IL	ME
MD	NC	VA	NH	NC	GA
NH	NJ	MD	MD	MD	WI
NC	IL	CENRAP	NC	ME	MD
VA	KY	ME	VA	VA	NC
WI	DE	TN	WI	TN	NH
GA	CENRAP	SC	TN	WI	MA
TN	WI	AL	NJ	NJ	TN
NJ	CT	WI	VT	GA	NJ
SC	GA	NH	GA	DE	AL
AL	TN	NJ	SC	SC	SC
DE	SC	DE	CT	AL	CT
CT	AL	CT	DE	CT	DE
VT	RI	MS	AL	RI	VT
RI	VT	RI	RI	VT	DC
MS	MS	VT	DC	DC	RI
DC	DC	DC	MS	MS	MS

Yet one more way of combining the ranked contributions is shown in Figure 8-2, which summarizes the relative contributions of four RPOs, Canada, and "outside domain" regions to ambient sulfate concentrations at several Class I areas using four different assessment techniques. The techniques considered here include: tagged REMSAD modeling, two CALPUFF platforms (MM5-based meteorology used by MDE and NWS observation-based meteorology used by VT DEC), the empirical emissions divided by distance approach (Q/d), and emissions times residence time probability. The estimates of state-by-state sulfate mass contributions ($\mu g/m^3$) from each method have been aggregated by RPO, both in terms of their absolute contribution (these values are displayed within the bars shown in the graphic) and in terms of their proportional contribution relative to other RPOs. It should be noted that the "outside domain"

contribution shown for each analysis method was derived exclusively from the REMSAD result. Averaging estimated impacts at the Acadia, Brigantine, and Lye Brook sites over the four assessment techniques utilized, MANE-VU states account for about 20 to 30 percent of sulfate impacts in these three MANE-VU Class I areas, while the Midwest RPO and VISTAS states each account for about 20 to 25 percent of the total sulfate contribution at Brigantine and Lye Brook and about 10 to 15 percent each at Acadia. The CENRAP states, Canada and "outside domain" add the remainder. Although variation exists across estimates of contribution for different sites and using different techniques, the overall pattern is generally consistent. Relative contributions are somewhat reversed at Shenandoah, which is a VISTAS Class I area. There, VISTAS states and Midwest RPO states account for roughly 20 to 30 percent of overall sulfate impacts, with MANE-VU states contributing roughly 15 to 20 percent.

Figure 8-2. Estimated RPO contributions to sulfate concentrations at Class I areas using different assessment techniques

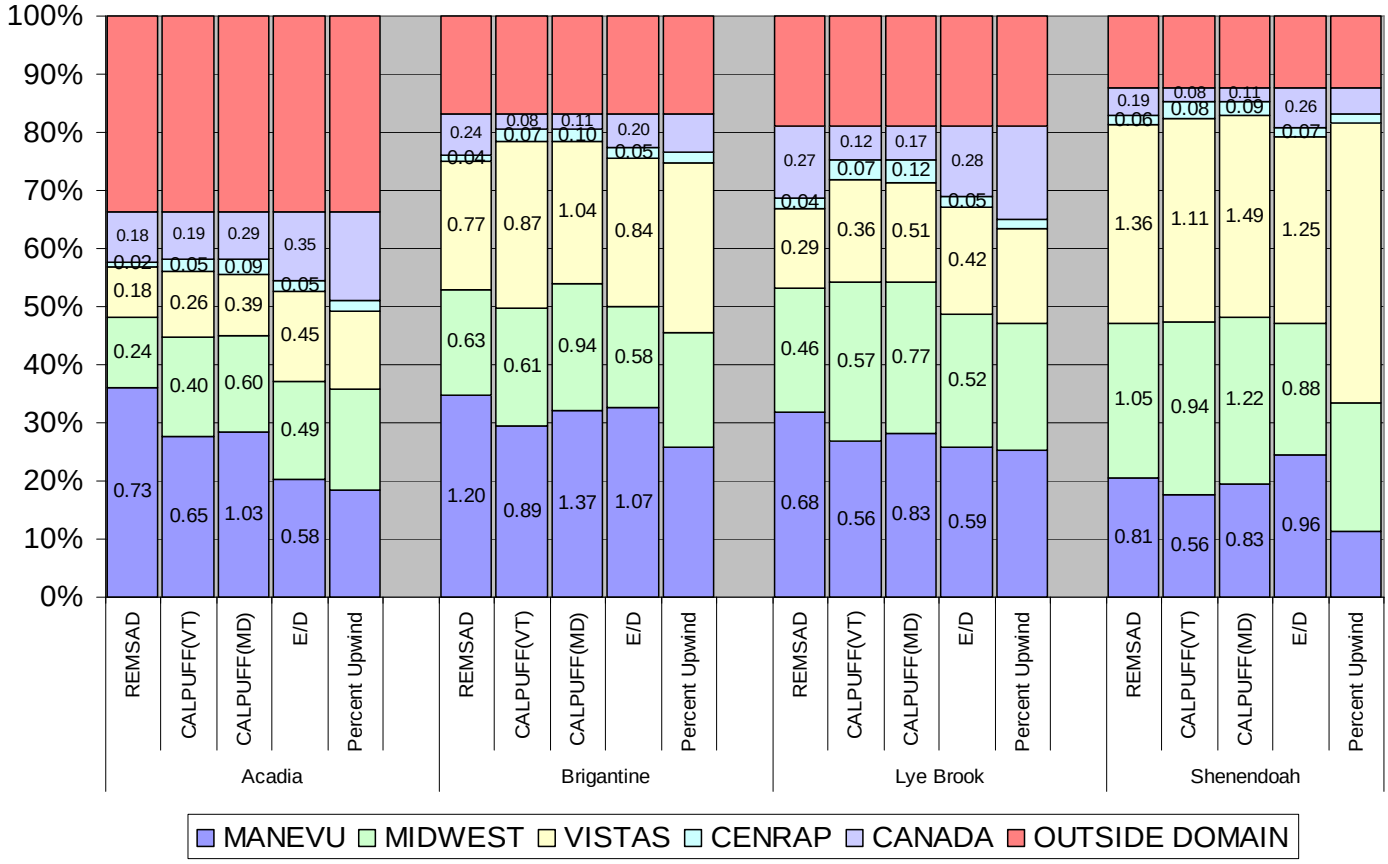

While the foregoing discussion has focused on quantitative methods for comparing contributions from individual states and regions, additional analyses have been conducted to verify and support these results using more qualitative means of identifying "regions of influence" for each Class I area. One such qualitative approach to synthesizing and interpreting the results obtained through different assessment techniques is illustrated in Figure 8-3 and Figure 8-4 below, which show a series of maps shaded to indicate different levels of contribution from different states and regions as determined by the analysis platforms already discussed. In these maps, states are shaded darker the higher they rank in terms of percent contribution to sulfate at a Class I site. For example, in Figure 8-3, states in a line from Indiana through Massachusetts are calculated to have the greatest impact on sulfate at Acadia. Overlaid on top of these maps are contours of

Figure 8-3. Ranked contributions of states to ambient sulfate concentrations at Acadia National Park, Maine.

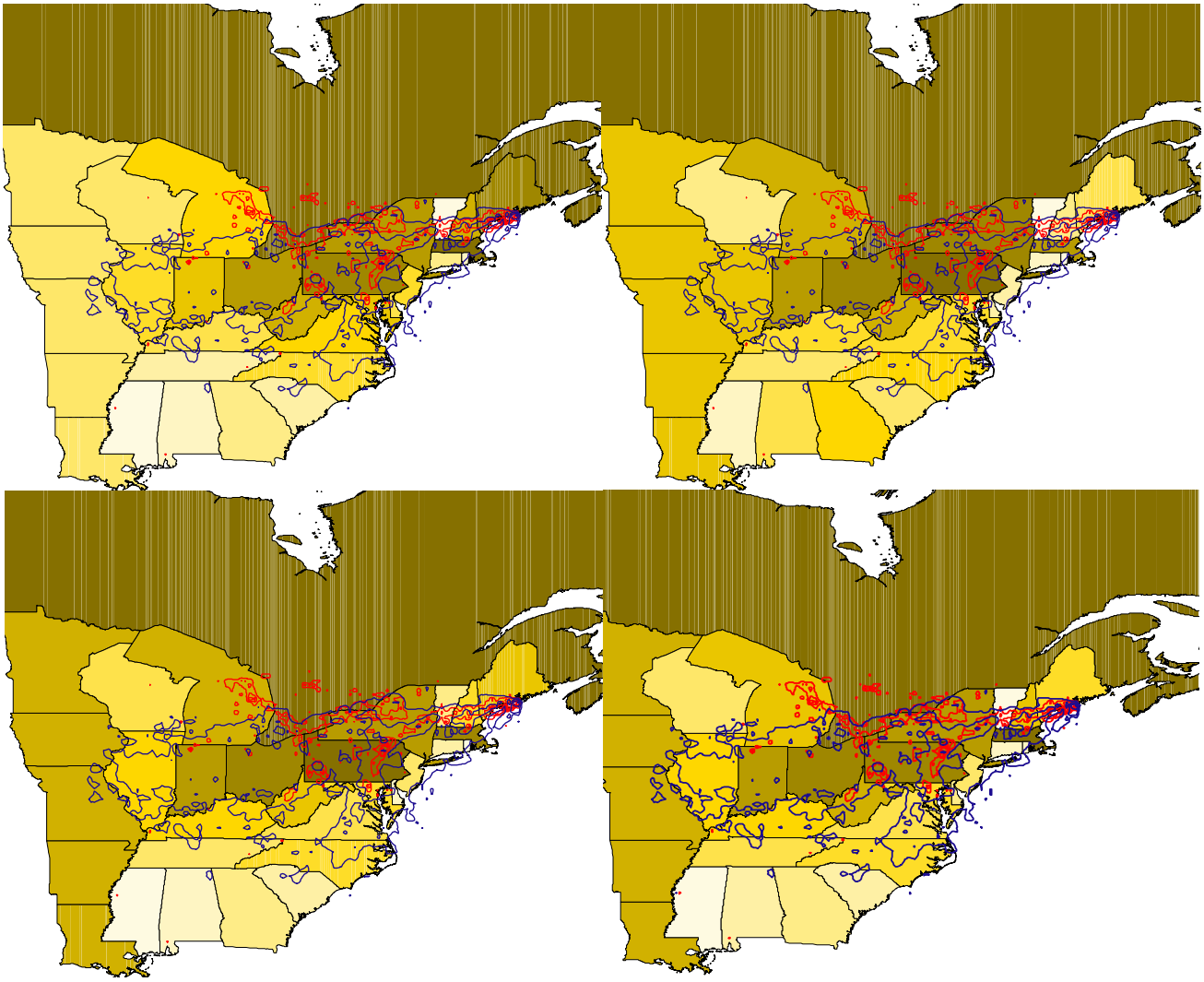

Note: Shaded maps show contributions as estimated by REMSAD, Emissions divided by Distance, CALPUFF VT, and CALPUFF MD. Red and blue contours representing regions of high incremental probability (IP) and high cluster-weighted probability (CWP) are overlaid onto the shaded state maps to indicate similarity of regional contributions as calculated by these independent receptor-based methods.

Incremental Probability (red) and Cluster Weighted Probability (blue) of contributing to sulfate on the highest days. The substantial consistency in the patterns support and bolster the quantitative results. The importance of this finding is that the receptor-based results portrayed by the contours rely on methods that are completely independent of the source-based modeling approaches used to calculate the underlying ranks. This sort of internal consistency among approaches gives considerable strength to the weight-of-evidence approach that MANE-VU has adopted for identifying sulfate source regions.

Figure 8-4. Ranked contributions of states to ambient sulfate concentrations at Brigantine Wilderness Area, New Jersey.

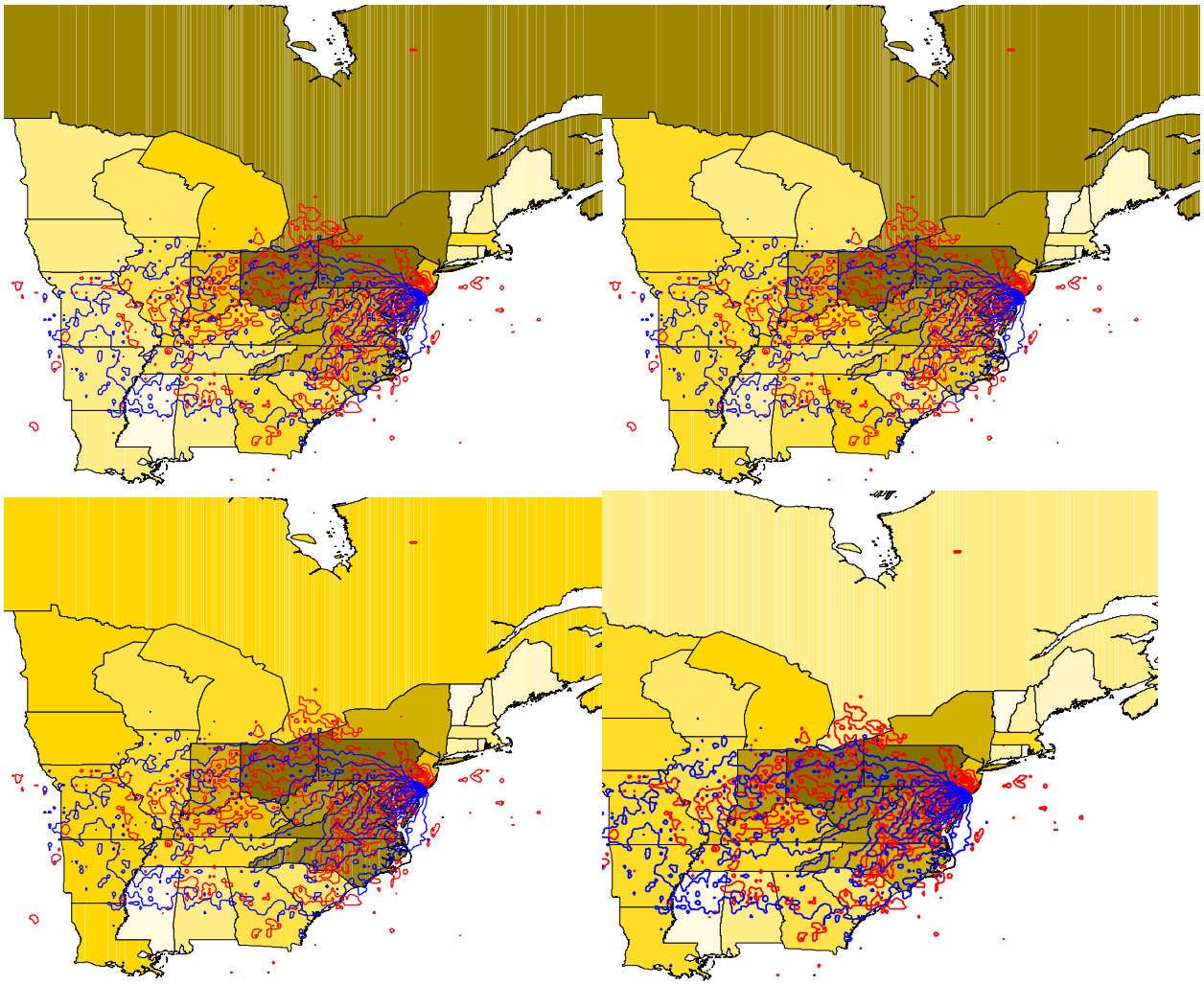

Note: Shaded maps show contributions as estimated by REMSAD, Emissions divided by Distance, CALPUFF VT, and CALPUFF MD. Red and blue contours representing regions of high incremental probability (IP) and high cluster-weighted probability (CWP) are overlaid onto the shaded state maps to indicate similarity of regional contributions as calculated by these independent receptor-based methods.

9. CONCLUSION

As MANE-VU prepares to implement the requirements of the Regional Haze Rule, a significant technical effort has focused on developing multiple analysis tools for assessing contributions to fine particle pollution and thus visibility impairment at Class I areas in the eastern United States. These analysis tools span the discipline of atmospheric science and include traditional Eulerian "source" or "grid" models, Lagrangian dispersion models, back trajectory receptor techniques, source apportionment models, and simple approximations based on empirical relationships between emissions and geography.

A review of the literature and of recent monitoring data has yielded a conceptual model of visibility impairment in the MANE-VU region that attributes a dominant role, on the worst visibility days, to the sulfate component of fine particle matter. This model in turn suggests that the most effective near-term strategy for reducing fine particle pollution and visibility impairment in the East is to continue reducing anthropogenic emissions of SO_2. Reductions in both NO_X and VOCs should also be considered. Given that sulfate, in particular, plays a dominant role in causing visibility impairment throughout the East, MANE-VU has focused on multiple methods of apportioning the sulfate mass found in ambient air at Class I sites to contributing states and regions. This weight-of-evidence approach is intended to overcome large uncertainties that would otherwise undermine confidence in the results obtained using any one modeling or analysis technique in isolation.

The assessment techniques described in this report use numerous approaches to develop ranked lists of individual state contributions to sulfate levels in MANE-VU Class I areas. When these results are normalized and compared, we find broad general agreement concerning the top contributing states at each site as well as some differences that suggest the magnitude of uncertainty inherent in these results.

The conclusions that emerge from this report regarding the relative contributions of different upwind RPOs to downwind sulfate concentrations at MANE-VU Class I areas appear quite robust and the modest differences presented here relative to the preliminary results presented in Spring of 2005 are a further indication that the general patterns of contribution presented here are unlikely to change due to further refinements of the emissions and meteorological inputs. This suggests that the MANE-VU findings are sufficiently robust to serve as a basis for inter-RPO consultations and the regional haze planning process. Given that as much as 30 to 50 percent of the ambient sulfate found at northeastern Class I sites on hazy days appears to originate within neighboring RPOs, coordination and consultation is likely to be critical if MANE-VU is to achieve its visibility goals for 2018 and beyond.

Appendix A: Application of Trajectory Analysis Methods to Sulfate Source Attribution Studies in the Northeast U.S.

Appendix B: Source Attribution by Receptor-Based Methods

Appendix C: Chemical Transport Model Results for Sulfate Source Attribution Studies in the Northeast U.S.

Appendix D: Development of Parallel CALPUFF Dispersion Modeling Platforms for Sulfate Source Attribution Studies in the Northeast U.S.